

1 **First spikes in visual cortex enable perceptual discrimination**

2 Arbora Resulaj^{1,2,3}, Sarah Ruediger^{1,2,3}, Shawn R. Olsen^{1,4}, Massimo Scanziani^{1,2,3}

3 1. Howard Hughes Medical Institute and Center for Neural Circuits and Behavior, University of
4 California San Diego, La Jolla, California 92093-0634, USA

5 2. Neurobiology Section and Department of Neuroscience, University of California San Diego,
6 La Jolla, California 92093-0634, USA

7 3. Department of Physiology, University of California, San Francisco, CA 94143, USA

8 4. Allen Institute for Brain Science, Seattle, WA 98103, USA

9

10

11 **Abstract**

12 Visually guided perceptual decisions involve the sequential activation of a hierarchy of cortical
13 areas. It has been hypothesized that a brief time window of activity in each area is sufficient to
14 enable the decision but direct measurements of this time window are lacking. To address this
15 question, we develop a visual discrimination task in mice that depends on visual cortex and in
16 which we precisely control the time window of visual cortical activity as the animal performs the
17 task at different levels of difficulty. We show that threshold duration of activity in visual cortex
18 enabling perceptual discrimination is between 40 and 80 milliseconds. During this time window
19 the vast majority of neurons discriminating the stimulus fire one or no spikes and less than 16%
20 fire more than two. This result establishes that the firing of the first visually evoked spikes in
21 visual cortex is sufficient to enable a perceptual decision.

22

23

24

25

26

27

28 **Introduction**

29 Perceptual decisions involve the sequential activation of several, hierarchically organized
30 cortical areas beginning with early sensory areas and ending with associational and motor
31 areas. Based on the number of areas likely involved in the processing of sensory stimuli it has
32 been hypothesized that in each area a relatively brief time window of activity may be sufficient
33 to enable a perceptual decision (Fabre-Thorpe, Richard & Thorpe, 1998). Yet, this time window
34 has never been directly measured for any specific area. By determining these lower limits and
35 analyzing neuronal activity over this time window within a given area we can establish the
36 minimal output of individual neurons in enabling perceptual decisions and reveal how the
37 stimulus is represented within this time frame in that area. Furthermore, this time window
38 defines the time that an area has to be active such that downstream areas can extract sufficient
39 information to enable a perceptual decision. How this time window relates to the time window
40 for an outside observer to extract sufficient information (Celebrini, Thorpe, Trotter, & Imbert,
41 1993; Mazurek & Shadlen, 2002; Shadlen & Newsome, 1998) is not clear.

42

43 The lack of answers to these questions is largely due to technical limitations. One key issue is to
44 demonstrate that the visual area of interest is necessary for the sensory discrimination task at
45 hand. Even though activity in a given area may carry relevant stimulus information, that area
46 may not be required for the perceptual decision. A second challenge is to precisely control the
47 duration of the sensory evoked response of that visual area. Answering this question has been
48 technically difficult since the duration of visually evoked activity in the brain cannot be precisely
49 controlled by the duration of the sensory stimulus. Even a stimulus as brief as 16 ms triggers a
50 response that lasts hundreds of milliseconds in visual cortex (Rolls, Tovee & Panzeri, 1999).
51 Presentation of a visual mask at various delays following the stimulus has been used to perturb
52 the long lasting neuronal response to a visual stimulus (Kovács, Vogels, & Orban, 1995; Lamme,
53 Zipser, & Spekreijse, 2002; Macknik & Livingstone, 1998; Rolls, Tovee, Purcell, Stewart, &
54 Azzopardi, 1994) and study the effects on perception. However, whether the impact on
55 perception is due to the suppression of the neuronal response to the stimulus or to the generation
56 of the neuronal activity by the mask (Macknik & Livingstone, 1998) is difficult to disambiguate.
57 Further, visual masks are not area specific but involve the entire visual system and thus cannot
58 address the minimal duration of activity of a specific visual area. In the mouse, optogenetic

59 approaches make it possible to selectively, rapidly and completely silence neuronal activity of a
60 given brain area (Lien & Scanziani, 2013; Olsen, Bortone, Adesnik, & Scanziani, 2012) at any
61 arbitrary delay after stimulus presentation (Reinhold, Lien, & Scanziani, 2015). With optogenetic
62 silencing we do not add activity but instead prevent activity from exiting the silenced area. With
63 this approach we can precisely control the duration of visually evoked activity in a cortical area
64 during a discrimination task.

65 Here we developed a simple visual discrimination task in mice that depends on visual cortex. By
66 completely and rapidly silencing primary visual cortex at well-defined intervals after the
67 stimulus appeared in the task, we demonstrate that this cortical area is required only during the
68 initial 80 ms from the onset of stimulus evoked response for a reliable decision to be made.
69 Importantly, during this period, most neurons in primary visual cortex fire one or no action
70 potentials. Thus, we establish the minimal time window of activity in primary visual cortex
71 sufficient to enable a perceptual discrimination and provide direct evidence for a key role of the
72 first action potentials fired by individual neurons in the execution of the task.

73

74 **Results**

75 **A visually guided behavior that depends on visual cortex**

76 To determine the minimal duration of activity in visual cortex necessary for accurate visual
77 discrimination by the animal, we needed to develop a perceptual task that requires visual cortex.
78 We developed a visual discrimination task in which mice are head-fixed yet free to run on a
79 treadmill (Figure 1A). Visual stimuli (circular patches of gratings oriented at different angles)
80 shown on a monitor placed on the right side of the animal (the antero-posterior body axis had a
81 15 degrees angle relative to the horizontal axis of the monitor with the axes converging rostrally)
82 moved horizontally from the anterior to the posterior end of the monitor at a speed that was
83 proportional to the running speed of the animal. One of the stimuli (a grating oriented at 90
84 degrees) was the target stimulus, while the other stimulus (a grating oriented at 45 degrees) was
85 the distractor. Stimuli appeared on the rostral edge of the monitor. Mice were rewarded with
86 water for bringing the target stimulus to the center of the monitor, the reward zone, and holding
87 it there for a minimum time set by the experimenter (~1s; a trial in which the stimulus is held in
88 the reward zone for at least the minimum time is called a “stop trial”; see Methods). To start the
89 next trial mice had to bring the stimulus out of the posterior end of the monitor and continue

running for some distance. To be most efficient in this task, mice had to continue running when the distractors appeared (Figure 1B). To ensure that mice did not solve the task by using local differences in contrast between the two gratings, we varied the position of the stripes in the circular patch, i.e. the spatial phase of the grating, randomly. At the beginning of each trial the stimulus appeared at the anterior end of the monitor and was frozen (i.e. insensitive to the rotation of the treadmill) for 350 ms, after which time the stimulus could be moved by the locomotion of the mouse. This ensured reproducibility of stimulus position across trials in the initial 350 ms. Mice learned to perform the task with accuracy above 85% correct in 23 ± 7 days (mean \pm std; n=15 wild type mice; Supplementary Figure 1; accuracy is defined as the average of the percentage of stop trials upon target presentation and the percentage of non-stop trials upon distractor presentation; chance level is 50%) completing on average 200 ± 30 trials each day (transgenic mice, VGat-ChR2-EYFP, learned the task in 50 ± 20 days, n= 8 mice; difference in learning rates was significant: p=0.0096, Wilcoxon ranksum test, Supplementary Figure 1).

To determine whether visual cortex (VC) is required for this visual discrimination task, we used two approaches: optogenetic silencing to determine the impact of an acute and reversible perturbation and surgical lesions to establish the effect of an irreversible ablation. We silenced cortical activity by optogenetically activating cortical inhibitory neurons (Atallah, Bruns, Carandini, & Scanziani, 2012; Lien & Scanziani, 2013; Olsen et al., 2012) with a 1 mm optic fiber placed over the left primary visual cortex (V1) (i.e. contralateral to the visual stimulus) in transgenic mice (VGAT-mhChR2-YFP) that selectively express the microbial light activated cation channel Channelrhodopsin2 (ChR2) in inhibitory neurons (Zhao et al., 2011) (Figure 1C). In these mice, V1 activity could be completely, rapidly and reversibly silenced (see Supplementary Figure 2) with a delay of 8 ms after the onset of illumination by a blue LED (450-490 nm, even at low powers of 3 mW) (Lien & Scanziani, 2013; Olsen et al., 2012). Cortical silencing started 76 ± 6 ms before the stimulus appeared (mean \pm std across mice) and ended just after the stimulus had exited the monitor, and was performed on a third of the trials interleaved randomly. During silencing trials the behavioral performance of mice was severely disrupted ($51 \pm 3\%$ accuracy; n=3 mice; Figure 1D). On these trials mice either kept on running no matter whether the target or distractor was presented (e.g. Figure 1D) or, on a fraction of trials, they sufficiently slowed down to center the grating (i.e. stop trial) but did so indiscriminately for both stimuli (p>0.16, Wilcoxon rank sum test on choice data; e.g. Figure 1D). Because the distinction between stop and non-stop trials is binary, i.e. based on a threshold

duration that the stimulus spends in the reward zone, it is conceivable that while performing at or close to chance when silencing cortex, mice may still hold the target for a longer time than the distractor in the reward zone. For example, targets and distractors may both spend less than the threshold time in the reward zone and hence be categorized as non-stop trials yet the targets may spend a longer time than the distractor in the reward zone. This would imply the ability of the mouse to discriminate despite performing at chance according to the criteria of the task. An advantage of our task is that it can reveal differences in the animal's behavior for target versus distractor that are not captured by the binary classification of stop versus non-stop trials. We thus verified that an ideal observer could not disambiguate the target from the distractor based on times spent by each of the two stimuli in the reward zone using receiver operating characteristic (ROC) analysis (see methods). The discrimination accuracy of the ideal observer was $55\pm6\%$ (mean \pm std, n=3 mice), hence very close to the actual performance of the task. (Figure 1D). To exclude the possibility that the optogenetic silencing simply distracted the mice from performing the task, we silenced the right visual cortex (i.e. ipsilateral to the visual stimulus) (Figure 1E). This manipulation resulted in no substantial impairment in the behavioral performance (88 \pm 6% accuracy for LED trials versus 89 \pm 6% for no LED trials; Figure 1E), thus showing that impairment was specific to the visual cortex processing visual information in the contralateral hemifield.

We verified that silencing visual cortex did not affect the ability of mice to express the decision, that is, to place the stimulus at the center of the monitor. Mice were trained as above but with the target stimulus only. In other words, mice where trained to perform a simple detection rather than a discrimination task. The distance that mice had to run to start the next trial was randomly varied. On trials where the contralateral visual cortex was silenced, mice centered the target image almost as frequently as in control trials (Figure 1F) demonstrating that visual cortex is not required to express the decision.

Behavioral deficits resulting from acute perturbations of the activity of a given brain area may lead to incorrect interpretations relative to the actual role of that area for behavior (Otchy et al., 2015), since following permanent lesions of said area animal's behavior can recover without additional training (Kawai et al., 2015). To further assess the necessity of VC in visual discrimination we trained mice to perform the visual discrimination task and, after they had reached proficiency (accuracy of 93 \pm 7%, n= 4 mice), we surgically removed VC contralateral to

154 the side of stimulus presentation (e.g. Figure 2A) and allowed the animals to recover for ten days
155 post-surgery before behavioral testing. Lesioned animals performed at chance ($p>0.3$, Wilcoxon
156 rank sum test on choice data, $n=4$ mice, Figure 2B). The impairment in behavioral performance
157 was not due to the ten day interval from the last behavioral session because trained control
158 animals experiencing even longer intervals between behavioral sessions remained proficient
159 (accuracy of $80\pm10\%$, Figure 2C). Furthermore the behavioral impairment was not due to either
160 anesthesia or to some unspecific impact of surgery because proficiency was preserved after
161 removing the ipsilateral VC (accuracy of 85%, $n=1$ mouse, Figure 2B) or following anesthesia to
162 perform craniotomy for physiological recordings ($80\pm10\%$, see results below). Taken together,
163 these results show that this visual discrimination task requires visual cortex.

164 **Neurons in primary visual cortex report stimulus identity by 80 ms**

165 To determine over what time interval stimulus evoked spiking activity in individual V1 neurons
166 can be used to disambiguate the target from the distractor stimulus we recorded extracellular
167 action potentials while the animals performed the task (Figure 3A). We inserted a multichannel
168 probe in V1 at the beginning of a behavioral session in trained mice (performance accuracy
169 during recordings: $80\pm10\%$, mean \pm std; $n = 9$ mice). To ensure that the units were maximally
170 excited by the stimulus, we placed the monitor so that the position of the stimulus in the initial
171 350 ms, when the stimulus is stationary, was superimposed on the multiunit spatial receptive
172 field (center of stimulus was 2 ± 1 degrees from center of receptive field, mean \pm std, $n=8$ mice).
173 The cortical response to the visual stimulus began 40 ± 5 ms after stimulus onset (mean \pm std
174 across mice, Figure 3C) consistent with previous reports (Niell & Stryker, 2008). The onset of
175 cortical response was quantified as the earliest deflection in the local field potential that
176 exceeded 3 standard deviations from baseline. We verified that the earliest deflection
177 corresponded to layer 4 of V1, the major thalamo-recipient layer, based on current source density
178 analysis (Niell & Stryker, 2008) (Supplementary Figure 3B).

179 To determine whether the spiking of an individual neuron allows an ideal observer to
180 discriminate the target from the distractor stimulus we performed ROC analysis (Tolhurst,
181 Movshon, & Dean, 1983) on 72 well isolated units in 9 behaving animals (Figure 3B,D-E; see
182 Methods for cell type and layer distribution). About half of the neurons (46%) discriminated the
183 target from the distractor when their activity was integrated over a time window of 300 ms,
184 starting at the onset the cortical response and ending just before the stimulus could be moved by

185 the animal (Figure 3E) ($p < 0.012$, Wilcoxon ranksum test on spike counts across trials,
186 Benjamini-Hochberg correction for multiple comparisons). Below we refer to these units as
187 “discriminating units”. How early do discriminating units start discriminating? We performed
188 ROC analysis at various intervals from the onset of the cortical response (Figure 3E). The
189 fraction of discriminating units increased rapidly between 40 and 80 ms (Figure 3F). While at 40
190 ms after the onset of the cortical response only ~20% of the discriminating units discriminated
191 the target from the distractor above chance, by 80 ms already ~ 50% of units did so with a
192 median discrimination accuracy of 66% (range: 58% - 79%). The fraction of discriminating units
193 discriminating increased more slowly following these initial 80 ms. By 300 ms (when, per
194 definition, 100% of discriminating units are discriminating) they reached a median
195 discrimination accuracy of 74% (range: 58% - 96%). Thus, already by 80 ms following the onset
196 of the cortical response ~50% of discriminating units discriminate the target from the distractor.

197 To determine how well the orientation tuning curve of a neuron predicts its ability to
198 discriminate we measured the tuning properties of discriminating neurons after the end of the
199 behavioral session. We presented drifting gratings of twelve different orientations that had the
200 same size and spatial frequency and were presented at the same location as the stimuli used
201 during the task, yet they were not rewarded and their location was insensitive to the movement of
202 the wheel (passive viewing; stimulus properties: 20°/s; 0.5s; 15° steps; chosen in a random order;
203 drifting in either of the two directions perpendicular to the grating’s orientation). Most
204 discriminating units that preferred the target during the task showed a peak response to
205 orientations larger than 90 degrees (109 ± 8 degrees, median \pm SEM; $n = 9$, 4 mice; Figure 3G).
206 Furthermore most discriminating units that preferred the distractor during the task, showed a
207 peak response to orientations less than 45 degrees (30 ± 20 degrees, median \pm SEM; Figure 3G;
208 $n = 8$, 4 mice). Non-discriminating neurons had either very sharp tuning curves peaking far away
209 from target and distractor orientations, or flat tuning curves, or tuning curves peaking in between
210 the target and distractor orientation (Supplementary Figure 4). We compared the difference in
211 spike number in response to grating presented at 45 and 90 degrees during passive viewing with
212 how well discriminating units distinguish the target from the distractor during the task. The
213 difference in spike number during passive viewing correlated with the value obtained from ROC
214 analysis over the initial 80 ms following the onset of cortical response during the task (R^2 based
215 on linear fit: 0.35; Figure 3H).

216 **The threshold duration of V1 activity for perceptual discrimination limits most neurons'**
217 **firing to one or no spikes.**

218 What is the minimal duration of activity in visual cortex necessary for accurate visual
219 discrimination? And how many action potentials are fired by individual neurons during this
220 time? If by 80 ms from the onset of visually evoked cortical activity information about stimulus
221 identity is available to an independent observer, it may also be available to the mouse. Thus, the
222 minimal duration of visual cortical activity enabling discrimination may be around 80 ms.

223 To control the duration of the visually evoked cortical response we optogenetically silenced
224 visual cortex, as described above, at varying intervals after the onset of the response (Figure 4A).
225 In each experiment we ensured that the LED intensity was sufficiently high such that
226 performance accuracy was at chance when the illumination started before the stimulus appeared
227 ($p>0.05$, Wilcoxon ranksum test on choice data, $n=8$ mice). Furthermore, as above, for each
228 animal we verified that despite chance performance the hold times of the stimulus in the reward
229 zone of the monitor did not differ between target and distractor stimulus ($p>0.05$, Wilcoxon
230 ranksum test on stimulus centering times in the reward zone). We verified this again at the very
231 end after testing all LED onset intervals.

232 The accuracy of the behavior increased with increasing interval between the onset of the cortical
233 response to the stimulus and the onset of cortical silencing (Figure 4B,C). When cortical
234 silencing followed the onset of cortical response by 44 ± 6 ms the performance was close to
235 chance ($54\pm5\%$; mean \pm std across mice, Figure 4D), similar to when the LED onset preceded
236 stimulus presentation ($51\pm3\%$; mean \pm std across mice). Strikingly, however, when cortical
237 silencing was delayed by a further 40 ms, hence with a latency of 80 ms after the onset of the
238 cortical response, performance accuracy of the animals sharply increased to $76\pm7\%$ (mean \pm std
239 across mice). Performance accuracy continued to increase, yet less sharply, over the longer
240 intervals tested reaching $92\pm5\%$ when the LED onset followed the onset of the cortical response
241 by 300 ms (mean \pm std across mice). With this interval the animals performed similarly to
242 control conditions, in the absence of LED illumination ($94\pm2\%$; mean \pm std across mice). Thus,
243 there is a sharp increase in performance when visual cortex is allowed to function between 44
244 and 80 ms after the onset of the cortical response. As above, we used ROC analysis to compare
245 behavioral performance with the ability of an ideal observer to disambiguate the target from the
246 distractor based on times spent by each stimulus in the reward zone when silencing cortex at 44

247 ms following the onset of the cortical response. The discrimination accuracy of the ideal
248 observer was $54\pm7\%$, hence very close to the actual performance of the task at 44 ms ($54\pm5\%$).
249 These results show that the minimal duration of visually evoked activity in V1 for an animal to
250 perform the present task above chance lies between 40 and 80 ms.

251 If the estimated time window indeed approximates the threshold duration of V1 activity for
252 perceptual discrimination, performance accuracy in trials when V1 is active for only 80 ms
253 should be very sensitive to the difficulty of the task. We thus trained mice to discriminate a
254 narrower angle difference between target and distractor, namely 15 degrees. Mice were first
255 trained to perform the standard 45 degrees discrimination task and their behavioral performance
256 measured across various intervals of cortical silencing, as above. We then re-trained those same
257 animals to discriminate a target from a distractor separated by 15 degrees until they reached a
258 similar level of proficiency as for the 45 degrees task (accuracy of $90\pm4\%$ for 15 degrees versus
259 accuracy of $93\pm2\%$ for 45 degrees, mean \pm std, n=3 mice, Figure 5B). We silenced the cortex of
260 these animals at various intervals following the onset of the cortical response and compared the
261 decrease in performance between the 45 and the 15 degrees discrimination tasks. Silencing
262 cortex at 80 ms after the onset of the cortical response reduced performance significantly more
263 for the 15 degrees as compared to the 45 degrees discrimination task in all animals ($p<0.05$,
264 Wilcoxon ranksum test on choice data, n=3 mice Figure 5B,C). While silencing V1 80 ms
265 following the onset of the cortical response still enabled the 15 degrees discrimination to occur
266 above chance ($p<0.02$, Wilcoxon ranksum test on choice data, n=3 mice), the accuracy was
267 significantly lower than for 45 degrees discrimination ($p<0.02$, Wilcoxon ranksum test on choice
268 data, n=3 mice, Figure 5B,C). This difference cannot be accounted for simply by a difference in
269 motivation or in control performance because in two out of three mice non-LED trials during the
270 15 degrees discrimination task were as accurate as non-LED trials during the 45 degrees
271 discrimination task (Wilcoxon ranksum test on choice data, p=0.65 and 0.67, Figure 5B). Thus,
272 these experiments demonstrate that the time between 40-80 ms following the onset of the cortical
273 response indeed captures the threshold duration of V1 activity for a simple perceptual
274 discrimination.

275 Over these initial 80 ms from the onset of the cortical response discriminating units in primary
276 visual cortex fired only $25\pm4\%$ of all the spikes fired above baseline during the 300 ms window
277 (mean \pm sem across units, Supplementary Figure 3D). During this 80 ms interval discriminating

278 units fired 0.6 ± 0.1 (median \pm SEM across units) action potentials in response to their preferred
279 stimulus (Figure 6F, response not different for the wild type and the transgenic mice as shown in
280 Supplementary Figure 3C), corresponding to a firing rate of 7.5 Hz, and 0.22 ± 0.06 action
281 potentials for their non-preferred stimulus. Furthermore, in response to their preferred stimulus,
282 discriminating units fired only 1 or no action potential in 80% of the trials and 2 action potentials
283 in only 11% of the trials (Figure 6E), similar to what is expected by Poisson statistics (% of
284 variance explained across units: $R^2 = 97 \pm 5\%$, median \pm SEM; median time until first action
285 potential: 70 ± 10 ms and 80 ± 20 ms from the onset of the cortical response for the preferred and
286 non-preferred stimulus, respectively (median \pm SEM across units; analysis performed over the
287 initial 300 ms from the onset of the cortical response, Figure 6C); mean latency difference: 12 ± 6
288 ms (mean \pm sem across units; $p = 0.03$; t-test; Figure 6D)). Thus, over the initial 80 ms from the
289 onset of the cortical response the vast majority of discriminating units in primary visual cortex
290 get to fire either one or no action potentials.

291 To determine whether indeed the first action potential in response to a stimulus is sufficient to
292 discriminate the target from the distractor we performed ROC analysis (Figure 6G) after
293 removing from each unit all but the first action potential after the onset of the cortical response.
294 As above we performed this analysis for various intervals from the onset of the cortical response.
295 The first action potential was sufficient for $\sim 33\%$ of units to discriminate by 300 ms (compared
296 to 46% if all the action potentials were available), and more than half of those units (54%) could
297 discriminate above chance at 80 ms (Figure 6H). Thus for most units the first action potential
298 substantially contributes to their ability to discriminate within the initial 80 ms after the onset of
299 the cortical response.

300 Finally, the accuracy of the behavioral response during the initial 80 ms can be explained by
301 pooling the activity of ~ 5 discriminating neurons on average (Supplementary Figure 5B), or ~ 20
302 neurons if non-discriminating neurons are also included in the pool (Supplementary Figure 5C).

303 Taken together, these results show that the threshold duration of visually evoked cortical activity
304 for a simple visual discrimination lies between 40 and 80 ms, a time window during which most
305 individual cortical neurons get to fire one or no spike.

306

307

308 **Discussion**

309 We have developed a visual discrimination task that necessitates visual cortex because both
310 acute cortical silencing and permanent ablation reduces performance of the task to chance. By
311 silencing visual cortex at various intervals following the onset of the cortical response we show
312 that the lower temporal limits of visually evoked activity for a perceptual discrimination lie
313 within 40-80 ms. The impact on behavioral performance when silencing visual cortex during this
314 time window is particularly sensitive to the difficulty of the task. Importantly, during this initial
315 80 ms window, most of the neurons in primary visual cortex that disambiguate the identity of the
316 stimulus fire either none or one action potential.

317

318 The simple detection of a stimulus can be reported by an animal in response to direct cortical
319 stimulation eliciting not more than one action potential in individual neurons (Histed &
320 Maunsell, 2013). Stimulus discrimination via cortical stimulation, on the other hand has been
321 reported only in response to repetitive stimulation eliciting series of action potentials (Romo,
322 Hernández, Zainos, & Salinas, 1998). We show that mice can discriminate visual stimuli even
323 when most neurons in visual cortex are prevented from firing more than their first action
324 potential. Thus, the first sensory evoked spikes of mouse visual cortical neurons are sufficient to
325 drive downstream areas for a reliable execution of the task. This highlights the ability of cortical
326 areas to instruct downstream targets with only a fraction of their neurons firing a single spike.
327 However, our data also clearly show that extending this time window increases (i) the animal's
328 behavioral performance, (ii) the ability of an ideal observer to disambiguate the stimulus based
329 on the spiking of individual neurons, and (iii) the fraction of neurons that can be used to
330 disambiguate. Extending the time window not only gives more neurons the opportunity to fire
331 their first spike (Figure 6C,D), but also enables second and third visually evoked spikes to
332 contribute to the discriminability of the stimulus (compare Figure 6G with Figure 3E).

333

334 The ability for a neuron to disambiguate two stimuli with only one or no spike depends on how
335 distinct the response of that neuron is for those stimuli and on the trial to trial variability of its
336 responses (Figure 3G,H). In mice, visual cortical neurons have orientation tuning functions with
337 relatively broad half widths at half max averaging 30-40 degrees. Given the large trial to trial
338 variability of visually evoked responses in cortical neurons, one may expect that as the difference

339 in orientation between the target and distractor stimuli become narrower, and the overlap in the
340 responses of individual neurons to different stimuli increases more spikes per neurons, or more
341 neurons spiking may be necessary to disambiguate the stimuli. As a consequence visual cortex
342 may need longer than 80 ms. Consistent with this, our results show that animals trained to
343 perform equally well on a 45 and 15 degrees difference discrimination task, are significantly
344 more impaired on the 15 degrees discrimination task when limiting V1 activity to 80 ms.

345

346 Prior work has investigated the minimal time window needed by an outside observer to extract
347 stimulus information from the neuronal activity of an area (Celebrini, Thorpe, Trotter, & Imbert,
348 1993; Mazurek & Shadlen, 2002; Shadlen & Newsome, 1998). How does the minimal time
349 window needed by an outside observer relate to the minimal time window that is sufficient to
350 enable a perceptual discrimination? Our analysis shows that an independent observer
351 accumulating spikes from around 100 neurons preferring the same stimulus would reliably
352 discriminate the target from the distractor within the initial 30 ms from the onset of the cortical
353 response (Supplementary Figure 5B). Because mice discriminate at chance when visual cortex is
354 only active for 40 ms, the minimal time window that downstream areas necessitate to extract
355 sufficient stimulus information is longer than the minimal time window necessitated by an
356 independent observer. This suggests that downstream areas integrate spikes over longer periods
357 than strictly necessary which may either be due to having to overcome noise (Mazurek &
358 Shadlen, 2002; Shadlen & Newsome, 1998) or unrelated changes, or having to first reconfigure
359 population activity before stimulus information can be integrated. Yet other explanations are
360 possible. Investigating these possibilities will require future identification of downstream areas
361 involved in the task and recordings of neural activity from these areas while visual cortex is
362 silenced. It must also be stated that the time window for the independent observer might be
363 slightly underestimated because neurons were pooled from different experiments and thus the
364 weak correlated noise which exists in simultaneously active neurons, and cannot be averaged out
365 by pooling to increase the signal to noise ratio (Zohary, Shadlen, & Newsome, 1994), is slightly
366 reduced.

367

368 What is the role of visual cortex in perceptual discrimination? Visual cortex is not necessary for
369 all visually guided behaviors in rodents. Several experiment have demonstrated that animals can
370 still perform visually guided behavior even following the silencing or ablation of visual cortex

371 suggesting the involvement of subcortical areas (Glickfeld, Histed, & Maunsell, 2013; Liang et
372 al., 2015; Petruno, Clark, & Reinagel, 2013; Prusky & Douglas, 2004). These behaviors
373 however, are either innate or, when learned, enable simple stimulus detection rather than
374 discrimination tasks. Some of these subcortical visual areas may indeed enable our mice to place
375 the stimulus in the center of the monitor while the cortex is silenced, yet other strategies are also
376 possible. Although we show that visual cortex is required to enable discrimination, consistent
377 with recent work (Jurjut, Georgieva, Busse, & Katzner, 2017; Poort et al., 2015), one may debate
378 whether visual cortex plays an instructive role by providing information disambiguating the
379 target from the distractor to downstream areas or simply a permissive role by regulating the
380 overall excitability of those downstream areas (Otchy et al., 2015). We show that permanent
381 ablation of V1 in trained animals reduces task performance to chance levels even ten days
382 following the lesion. This result differs from what is observed after lesioning motor cortical areas
383 on specific motor tasks (Kawai et al., 2015). While acute silencing of these motor cortical areas
384 impairs behavior, following permanent ablation of these same areas behavior is regained within a
385 few days without further training (Otchy et al., 2015). As a consequence these motor areas are
386 considered permissive rather than instructive for the execution of the behavior (Otchy et al.,
387 2015). Instead, given the absence of recovery, our ablation results are consistent with an
388 instructive role of V1. Clearly, we cannot exclude the possibility that the hypothetical area
389 downstream of V1 simply does not recover its original excitability without V1. However, the
390 fact that on the one hand the animal behaves at chance upon silencing cortex before the stimulus
391 presentation, rather than being only partially impaired, and on the other hand that just 80 ms of
392 activity are sufficient to almost completely recover the behavior is further evidence, in our
393 opinion, for an instructive role of visual cortex. The sufficiency of a sensory cortical area to elicit
394 a perceptual decision has been demonstrated for the somatosensory (O'Connor et al., 2013;
395 Romo et al., 1998) and taste (Peng et al., 2015) systems and controlled perturbations of visual
396 areas has been shown to affect decision (Salzman, Britten, & Newsome, 1990) in a predictable
397 manner. The ability to artificially recapitulate the pattern of cortical activity elicited by a visual
398 stimulus through direct cortical activation will eventually provide a definite answer (Häusser &
399 Smith, 2007).

400 It is not clear whether our findings may generalize to the phenomenon of visual masking in
401 which a second stimulus presented shortly after the first may render the first stimulus less visible
402 or invisible. The neural mechanisms underlying visual masking, that is how added activity from

403 two stimuli generates the perceptual illusion of masking, are not well understood (Breitmeyer,
404 2007; Macknik & Livingstone, 1998). In the current study we address the simpler and more basic
405 question of the minimal duration of activity in response to a single stimulus still able of
406 triggering a perceptual decision. Indeed there are clear differences between visual masking and
407 the optogenetic approach used here: First, our approach silences neuronal activity while visual
408 masking adds activity (Macknik & Livingstone, 1998). Second our approach is areas specific
409 while visual masking impact the whole visual system. Finally, we can silence visual cortex after
410 most neurons have fired one or no spikes in response to the visual stimulus while, during visual
411 masking experiments, even the just perceivable stimuli elicit multiple spikes (Kovács et al.,
412 1995; Lamme et al., 2002; Rolls et al., 1999). Future experiments using optogenetic approaches
413 may help us understand the neuronal mechanisms underlying the perceptual illusion of visual
414 masking.

415

416 We have provided direct evidence for the minimal amount of time that it takes visual cortex to
417 process visual information in order to enable a perceptual decision and determined the neuronal
418 activity that occurs during that period. The speed at which humans are able to discriminate visual
419 stimuli has led to the suggestion that processing of the visual stimuli can be accomplished with
420 individual neurons in each of the relevant brain areas firing either none or one action potential.
421 This work demonstrates that a period of activity in mouse primary visual cortex during which
422 most neurons fire none or one action potential is indeed sufficient to enable perceptual
423 discrimination. Future work will elucidate which downstream brain areas read out these first
424 essential spikes generated in V1.

425

426

427

428

429

430

431

432

433 **Materials and Methods**

434 **Animals.** All experimental procedures were approved by the University of California San Diego
435 Animal Care and Use Committee. Mice were on a 12h light/dark cycle, lights on at 8 pm.
436 Training and experiments were performed during the dark cycle. Mice were single-housed. Data
437 were collected from C57BL6 mice (Charles River Laboratories) or for optogenetic silencing,
438 VGat-ChR2-EYFP mice (Jackson Laboratories; stock number: 014548). All mice were male and
439 adults (2-5 months old) at the start of experiments.

440 **Surgery. Headbar implantation:** Each animal was implanted with a custom made headbar for
441 head-fixation. Briefly, animals were anesthetized with 2.5% isoflurane. Body temperature was
442 controlled by a thermal blanket connected to a rectal thermometer (FHC; DC Temperature
443 Controller). To expose the skull, the skin and periosteum were removed. The gap between the
444 edge of the skull and skin was sealed with Vetbond (Fisher Scientific). The headbar was affixed
445 to the skull with Krazy glue. Dental cement (Lang Dental; Ortho-Jet BCA) was mixed with black
446 ink and applied to reinforce the affixation of the headbar. Animals were allowed to recover for at
447 least 3 days before the start of water restriction (1 ml/day). **Craniotomy:** On the day before the
448 extracellular recording, animals were anesthetized as above and a craniotomy was made over V1
449 (size: 400 μ m x 1 mm, anterioposterior x mediolateral, center approximately 2.3 mm from
450 midline and 1.3 mm from lambdoid suture). At the end of the craniotomy, to protect the brain the
451 craniotomy was covered with a drop of artificial cerebrospinal fluid (ACSF; 142 mM NaCl,
452 5mM KCl, 10 mM D-glucose, 10 mM Hepes, 3.1 mM CaCl₂, 1.3 mM MgCl₂) and Kwik-Cast
453 (WPI). **Cortical Ablation:** The animals were anesthetized as above. Using stereotaxic coordinates
454 the outline of visual cortex (from Paxinos and Franklin mouse brain atlas (Paxinos & Franklin,
455 2007)) was marked at the surface of the skull. Using a dental drill (700 μ m) the area of visual
456 cortex was thinned and removed. Sterile PBS was used to hydrate the exposed brain area. A cut
457 of 1 mm depth was performed around the outline of VC using a microsurgical blade (FST). The
458 cortical tissue was removed using a spoon shaped microsurgical blade (FST 10317-14). The area
459 was washed with PBS to remove blood and consequently covered with Silicon Kwik-Cast (WPI).
460 Upon polymerization a layer of cyanoacrylate glue was applied to cover the lesioned area. An
461 additional layer of dental cement was applied to permanently cover the lesioned site.

462

463 **Behavioral Setup.** A schematic of the setup is shown in Figure 1A. Mice ran on a custom made
464 flat transparent disc, or wheel (diameter: 15 cm). The wheel was mounted on the shaft of a rotary
465 encoder (MA3-A10-125-B, US Digital), which provided an analog output voltage proportional to
466 the absolute shaft position. The encoder was mounted via an adaptor to a small Noga arm (MSC;
467 part number: 09560459). Data were acquired with a National Instruments data acquisition board
468 (NI USB-6009). To deliver water (~10 µl/reward) we used gravitational flow under the control
469 of a solenoid valve (NResearch; Model 161K011; valve driver: CoolDrive). The valve was
470 connected to a lickspout (hypodermic tubing; gauge 14) via Tygon tubing (1/16 inch ID).

471 **Visual stimulation.** Visual stimuli were presented on an LCD monitor (20.5x11.5 inches,
472 1920x1080 pixels, 60 Hz refresh rate, gamma corrected mean background luminance: 47 cd/m²
473 for optogenetic silencing for 6 mice and 120 cd/m² for 2 mice, and 110 cd/m² for
474 electrophysiology). The anterior edge of the monitor was positioned 25 cm from the right eye
475 and the monitor subtended 50 degrees to 150 degrees of the visual field. During the recording,
476 the monitor was moved slightly so that the stimulus when stationary, i.e. in the first 350 ms
477 (Figure 1A), overlapped with the multiunit spatial receptive field (see ‘Extracellular
478 Electrophysiology’). To quantify how well the stimulus was centered relative to the center of the
479 receptive field, at the end of the recording session we presented black and white squares of 3.6°
480 in a grid of 9x9 locations (one stimulus at a time) covering the whole stimulus area for 4 mice
481 and squares of 6° in a 5x5 grid for 4 mice. The stimuli were generated using PsychToolbox
482 (Brainard, 1997) and custom written software in Matlab (Mathworks).

483
484 For the behavioral task, stimuli were circular patches of static sinusoidal gratings (spatial
485 frequency: 0.146 cycles/degree, diameter: ~30°, contrast: 50%). On each trial, the spatial phase
486 of the grating was chosen randomly out of 7 evenly spaced phases. We monitored the timing of
487 stimulus onset by placing a photodiode (response time 15 ns; PDB-C156-ND; Digikey) at the
488 bottom anterior part of the monitor, where a white square appeared concurrently with the
489 stimulus after a 5 ms delay (accounted for in our analysis). The horizontal motion of the stimulus
490 was controlled by the running of the animal, and updated at ~20 Hz (monitor refresh rate: 60
491 Hz). The gain, defined as stimulus displacement on the monitor (cm)/ running distance (cm)
492 varied from 0.3-0.6 across animals depending on how fast each animal ran (Supplementary Table
493 1). The distance between two consecutive stimuli in the track was 1.25 times the width of the
494 monitor.

495 For the recording sessions, the spatial phase of the grating was constant and did not vary trial to
496 trial. During passive viewing (Figure 3G,H and Supplementary Figure 4), the stimuli had the
497 same size and spatial frequency and were presented at the same location as the stimuli used
498 during the task during the initial 350 ms, yet the stimuli were not rewarded and their location was
499 insensitive to the movement of the wheel (passive viewing). We presented drifting gratings of
500 twelve different orientations (3 Hz thus 20 degrees/s; 0.5s; 15° steps; chosen in a random order;
501 drifting in either of the two directions perpendicular to the grating's orientation). The duration of
502 the inter trial grey screen was 0.75 sec. We presented ~ 30 repetitions/direction. The size and
503 spatial frequency of the stimulus as projected on the retina will vary depending on its position on
504 the monitor. However data on electrophysiological recordings only report activity for a specific
505 position of the stimulus on the monitor, when the stimulus is fixed. This position is the same for
506 stimuli presented during the task and during passive viewing.

507 **Photo-activation of cortical interneurons to silence V1.** An optical fiber (1 mm) coupled to a
508 blue LED (470 nm; Doric Lenses) was placed over V1 above the intact skull covered with a thin
509 layer of Krazy glue. The fiber was placed at approximately the retinotopic location corresponding
510 to the stimulus during the initial 350 ms in the task: ~2.3 mm from midline and ~1.3 mm from
511 lambdoid suture. To find these coordinates, we recorded multiunit activity in V1 with the
512 monitor in the same position as during optogenetic silencing (monitor was moved <15 degrees to
513 center the spatial receptive field of the multiunit activity). We used these same approximate
514 coordinates for all of our recordings.

515 For each animal, the total power was increased until the performance was at chance level when
516 the LED illumination started before the stimulus appeared (3.3 - 20 mW across animals; p>0.05;
517 Wilcoxon ranksum test on stimulus centering times in the reward zone). To turn the LED on at
518 specific delays after stimulus onset, the photodiode signal detecting the onset of the stimulus was
519 sent to an amplifier (Newark; TWLUX - TW-MF2CAB) and then to an external microprocessor
520 (Mega 1280; Arduino). The microprocessor waited for the amplified photodiode signal to cross a
521 threshold before sending out a digital trigger to the LED driver (Thorlabs). The jitter (s.d.) of the
522 LED onset was 4 ms.

523 **Behavioral training.** Training began after animals had been on water restriction for at least 7
524 days (~1 ml water/day). During training, mice were kept at 80% or above of their initial body
525 weight. Additional water was provided if the body weight fell below 80% of the initial weight.

526 The initial behavioral parameters were: 100% contrast, gain (gain= stimulus displacement in the
527 monitor (cm)/ running distance (cm)): 0.6, hold time (minimal time in reward zone for a reward):
528 0.2s. With these parameters, mice would get a water reward every time a new target stimulus
529 would pass the reward zone, i.e. as long as they kept running. After mice began to run
530 consistently (one to a few sessions), the gain was decreased to 0.45 and the hold time was
531 initially increased to 0.4 sec to get the first ~10 rewards each session (i.e. during the warm up
532 period) and then increased to 0.9 sec. Mice learned to perform the task, that is to hold the target
533 in the reward zone for at least the minimal hold time for a reward, but not the distractor, with
534 accuracy >85% in 23 ± 7 days (mean \pm std; n=15 wild type mice) completing on average 200 ± 30
535 trials each day (transgenic mice learned the task in 50 ± 20 days, Supplementary Figure 1). Over
536 this period, if mice were running too fast and not stopping on a substantial fraction of targets, the
537 gain was decreased (lowest value: 0.3). Conversely, if mice were stopping on a substantial
538 fraction of distractors, the hold time was increased (up to a value of 1.5 sec). After mice achieved
539 ~ 85% accuracy, stimulus contrast was decreased to 50%. Mice easily generalized to stimuli of
540 50% contrast.

541 The animal's discrimination accuracy based on the binary classification of stop versus non-stop
542 trials could be lower than that of an ideal observer monitoring the time that the stimulus spends
543 in the reward zone. This could be the case if, for example, on some target trials the mouse slows
544 down more than it would for a distractor trial but not sufficiently so for the target to spend the
545 minimal amount of time in the reward zone and hence be classified as a stop trial. This scenario
546 would lead to an underestimate of the animal's ability to discriminate. For cortical silencing,
547 when the LED illumination started before the stimulus appeared, the animal's discrimination
548 accuracy was similar to that of an ideal observer based on ROC analysis of the stimulus
549 centering times in the reward zone. However, when the LED illumination started after the
550 stimulus appeared, particularly for intervals longer than 80 ms from onset of the cortical
551 response, the animal's discrimination accuracy was usually noticeably lower than that of an ideal
552 observer (>10% difference). This difference would often occur because on some target trials
553 mice would not slow down sufficiently for the trial to be a 'stop trial' but they would slow down
554 more than they would for distractor trials. Thus, an advantage of our task is that it revealed
555 differences in the animal's behavior for target versus distractor that were not captured by the
556 binary classification of stop versus non-stop trials.

557 To motivate mice to make choices with similar accuracy to that of an ideal observer monitoring
558 the time that the stimulus spends in the reward zone, we adjusted the probability that an image
559 would be a target and the minimum time that the target had to be centered for a reward (hold
560 time). Decreasing target probability increases the gap between rewards. With decreasing
561 probability of the image being a target, any miss is accompanied by a longer average time
562 interval until the next target arrives. Similarly, as the probability of the image being a distractor
563 increases, a given false alarm rate increases the average time until the next target is
564 available. The parameters were adjusted until for LED illuminations starting 301 ms after
565 cortical onset (Figure 3) mice made choices that had an accuracy similar to that of an ideal
566 observer (difference did not exceed 7%). Adjusting parameters for the longest interval between
567 the onset of the cortical response and the LED illumination (301 ms) was usually sufficient for
568 the discrimination accuracy by the animal to be similar to that of an ideal observer for shorter
569 intervals too. For data collection, parameters were kept constant across different intervals. For a
570 list of final parameters for all mice included in the main experiments see Supplementary Table 1.
571 The probability that a stimulus would be a target varied from 25%-50% across mice, and the
572 hold time varied from 0.6s – 1.0s across mice. Each interval was tested for 1-3 sessions totaling
573 130 ± 70 trials (range: 42-372 trials per interval), and data were pooled together for analysis.

574 **Extracellular Electrophysiology.** On the day of the recording the Kwik-Cast was removed,
575 ACSF was added and, before the recording electrode penetrated the brain, a drop of 1% agarose
576 (Type IIIA; Sigma-Aldrich) was added to reduce movement artifacts. The recording electrode
577 was a NeuroNexus 32 channel linear probe (A1x32-Edge-5mm-20-177) that span 620 μm in
578 depth across cortical layers. The probe was inserted approximately perpendicular to pia and
579 lowered to a depth of ~ 850 -900 μm (the curvature of the V1 surface was estimated using the
580 Franklin and Paxinos brain atlas (Paxinos & Franklin, 2007)). The probe was connected with a
581 Plexon adaptor to two 16-channel A-M Systems headstages (gain 20x) and then connected to two
582 16 channel A-M Systems amplifiers (Model 3600; gain: 500x, high pass filter: 0.3 Hz, low pass
583 filter: 5 kHz). The voltage signals were acquired with a National Instruments data acquisition
584 board and extracted with custom written software in Matlab.

585 Data collection began at least 30 min after insertion of the probe. We first presented black or
586 white squares of $\sim 10^\circ$ to map the location of the receptive field across all channels of the probe.
587 To ensure that all receptive fields overlapped with the stimulus position during the behavior in

588 the first 350 ms of a trial (Figure 1A), we either moved the monitor slightly if the movement was
589 approximately $<15^\circ$, or reinserted the probe at a different location mediolaterally. We mapped
590 the receptive field at a higher spatial resolution at the end of the recording for 8 mice (for same
591 units and same stimulus and monitor position, see ‘Visual Stimulation’).

592 **Histology:** Mice were transcardially perfused with 4% paraformaldehyde (PFA) in PBS. The
593 brain was post-fixed in 4% PFA overnight in 4°C and then cut in 100 μm thick coronal sections
594 using a vibratome. To estimate the extent of the lesion, consecutive sections were used. All mice
595 had lesions in V1 and surrounding V2 areas. The lesion extended slightly into the following
596 areas (as outlined in the Paxinos and Franklin mouse brain atlas (Paxinos & Franklin, 2007)):
597 hippocampus (2/5 mice), retrosplenial cortex (2/5 mice), primary somatosensory cortex (2/5
598 mice), primary and secondary auditory cortex (1/5 mice), temporal association cortex (1/5 mice),
599 parietal association cortex (2/5 mice), dorsal subiculum (1/5 mice), postsubiculum (2/5 mice).
600

601 **Data analysis: behavior.** We visualized the positioning of the stimulus on the monitor by
602 plotting the position of the leading (caudal) edge of the stimulus (Figures 1 and 3). A stop trial is
603 defined as the stimulus spending \geq the minimal time for reward in the reward zone (500 pixels
604 wide). Error bars in stop probability (Figures 1, 2, 4 and 5) indicate 95% confidence intervals
605 assuming a binomial distribution of stops and non-stops at each orientation (data pooled from all
606 sessions that each condition was tested). Accuracy for the target stimulus is defined as the
607 percentage of stop trials upon target presentation; accuracy for the distractor stimulus is defined
608 as the percentage of non-stop trials upon distractor presentation. Overall accuracy is taken as the
609 average of these two choice accuracies; chance level is 50% correct.

610 **Data analysis: spike sorting.** We used UltraMegaSort (Fee, Mitra, & Kleinfeld, 1996; Hill,
611 Mehta, & Kleinfeld, 2011) to sort spike waveforms into clusters. We then manually sorted the
612 clusters into putative units. Units were accepted as well isolated according to the following
613 criteria. First, the spike waveform across 4 channels had to be different than that of neighboring
614 units in the cluster. If there were similarities, the orientation tuning curves had to be different
615 otherwise the units were merged. Second, the refractory period violations for each unit did not
616 exceed 0.1% (except for Figure 2 where threshold was 0.2%). To reach this criteria, we
617 occasionally removed outliers (Hill et al., 2011) identified using the distribution of the
618 Mahalanbois distance of spike waveforms from the cluster center. Third, for each unit, the
619 fraction of spikes with amplitudes below detection threshold (4 s.d. of high frequency noise) did

620 not exceed 15% (including any removed outliers) as estimated by a Gaussian fit to the
621 distribution of spike amplitudes. Finally, we ensured that the spike waveform was stable for the
622 duration of trials in our analysis.

623 Out of 98 well isolated units ($n = 9$ mice, 1 recording/animal), 12 units (12%) were putative
624 inhibitory units based on spike waveform (Supplementary Figure 2). Isolated units spanned all
625 cortical layers.

626 **Data analysis: electrophysiology.** To estimate the onset of the cortical response (Figure 3C), we
627 first averaged for each channel the raw voltage traces across trials. We then filtered the averaged
628 trace (4th order Butterworth filter, low pass frequency cutoff: 300 Hz, applied bidirectionally) to
629 get the local field potential. The filtered trace was almost indistinguishable from the raw trace
630 (blue versus black, Figure 3C). The onset of the cortical response was defined as the earliest
631 deflection in the filtered traces exceeding 3 s.d. from baseline. The baseline was computed for
632 each channel as the average over the interval -80 ms to 20 ms from stimulus onset.

633 The current source density analysis based on the averaged traces was computed as described
634 before (Niell & Stryker, 2008; Reinhold et al., 2015). For the average CSD across mice in
635 Supplementary Figure 3B, 3 mice were excluded because either the recording electrode did not
636 span the same depth of cortex as other recordings ($n=1$ mouse) or there was noise in a few
637 channels ($n=2$ mice); both cases would lead to discontinuities in the average CSD if included.

638 To quantify for each recording how far the center of the receptive field was from the center of
639 the stimulus, at each stimulus location (black or white squares in a 9x9 grid in 4 mice and 5x5
640 grid in 4 mice covering the whole stimulus area; see 'Extracellular Electrophysiology') and for
641 each channel we calculated the baseline subtracted response over a window of 170 ms (stimulus
642 duration: 120 ms), and then normalized the responses to the peak response. After, for each
643 location we averaged the responses across all channels. We then computed for each location the
644 average of the average response to the white squares and the average response to the black
645 squares. Lastly, we estimated the center of the receptive field by calculating the center of mass
646 from the average responses at different locations. The distance from the center of the receptive
647 field to the center of the stimulus was 2 ± 1 degrees (mean \pm std, $n=8$ mice).

648 We computed the area under the receiver operating characteristic (ROC) using a custom written
649 script in Matlab (same results were obtained using function *perfcurve* in Matlab). To exclude the

650 possibility that this analysis was not sensitive enough for low firing units, out of 98 well isolated
651 units, 13 (all regular spiking) were excluded because they fired < 1 spike every 6 trials over the
652 initial 300 ms. This threshold was chosen because units firing at rates just above this threshold
653 could discriminate ($p < 0.012$; Wilcoxon ranksum test comparing the distributions of the number
654 of action potentials for target versus distractor). We confirmed that the distribution of running
655 speeds for the two stimuli was not significantly different in the initial 350 ms and thus did not
656 affect our ROC analysis ($p > 0.02$, Wilcoxon ranksum test using the Benjamini-Hochberg
657 correction for multiple comparisons, $n = 9$ mice).

658 To determine how many neurons are needed to explain behavior, we first artificially increased
659 the number of units by randomly shuffling the trials of each unit to get 6 new units. We increased
660 the total number of units to 231 units for the pool containing discriminating units only and 504
661 units for the pool containing both discriminating and non-discriminating units. We then
662 randomly picked N units, where N was 2, 5, 10, 20, 50, 100, or 200. For all units preferring the
663 distractor, we switched the target responses with the distractor responses. Next we created a
664 'pooling neuron' that had for each trial all the spikes of all N neurons. We then performed ROC
665 analysis on the spikes of this pooling neuron. We repeated the random sampling step 1000 times
666 and averaged the resulting areas under the ROC curve. We repeated the whole procedure 10
667 times. Error bars in Supplementary Figure 5 are sem from these 10 repetitions.

668 To compute the time of the first spike for the preferred versus the non-preferred stimulus (Figure
669 6 B-D) we quantified for each unit the time of the first spike for each trial over the initial 300 ms
670 following the onset of the cortical response. For each unit we then normalized the distribution of
671 these spike times (total number of spikes = 1) and then averaged across units the fraction of
672 spikes in each time bin (20 ms bins, Figure 6C). We also show the mean of the spike times for
673 each unit and the distribution of these means across units (Figure 6D). To assess whether the first
674 spike occurred earlier for the preferred versus the non-preferred stimulus, for each unit we
675 computed the difference in the mean time of the first spike for the preferred versus the non-
676 preferred stimulus and tested whether the mean of the differences from all units was different
677 than zero (Student's t-test).

678 To compute orientation tuning curves, the firing rate for each orientation was calculated over the
679 initial 330 ms following cortical onset (i.e. the first cycle of presentation), averaged across
680 repetitions, and normalized by the maximal firing rate across orientations.

681 To compute the preferred orientation for each unit, we used the following equation (Lien &
682 Scanziani, 2013):

683
$$x = \sum r_k \cos(2\theta_k); \quad y = \sum r_k \sin(2\theta_k)$$

684 Preferred orientation = $0.5 \times \arctan(y/x)$ if $x > 0$

685 Preferred orientation = $0.5 \times (180 + \arctan(y/x))$ if $x < 0$

686

687 We computed orientation selectivity index (OSI) using the equation (Lien & Scanziani, 2013):

688
$$OSI = \frac{\sqrt{(\sum r_k \sin(2\theta_k))^2 + (\sum r_k \cos(2\theta_k))^2}}{\sum r_k}$$

689 To evaluate the dependence of the area under the ROC curve over the initial 80 ms after cortical
690 onset during the task versus the difference in the number of action potentials in response to
691 passively viewed stimuli of 45° and 90°, we fitted a linear function using least squares estimation
692 (Dobson & Barnett, 2008). The standard errors of the slope and offset parameters of the fit were
693 based on the inverse of the information matrix (Dobson & Barnett, 2008). The slope was
694 significantly larger than 0 ($p < 0.05$; t-test).

695 **Statistical analysis.** The stated p-values are the results of the Wilcoxon ranksum test unless
696 otherwise noted. For medians, we report standard errors calculated using bootstrapping.

697

698

699

700

701

702

703 **Author Contributions**

704 A.R. and M.S. designed the study. S.R. performed lesions of visual cortex. S.R.O developed the
705 behavioral task. A.R. performed experiments and analyzed the data. A.R. and M.S. wrote the
706 paper.

707

708 **Acknowledgements**

709 We thank J. Evora for help with mouse husbandry, Jeffery Isaacson, Lindsey Glickfeld and
710 Michael Shadlen for comments on the manuscript, Maria Dadarlat and members of the Scanziani
711 lab and Isaacson lab for helpful discussions, and Satoru Miura and Guy Bouvier for headbar
712 implantations on a subset of animals. This project was supported by the Gatsby Charitable
713 Foundation and the Howard Hughes Medical Institute.

714

715

716

717

718

719

720

721

722

723

724

725

726

727

728 **References**

- 729 Atallah, B. V., Bruns, W., Carandini, M., & Scanziani, M. (2012). Parvalbumin-expressing
730 interneurons linearly transform cortical responses to visual stimuli. *Neuron*, 73(1), 159–170.
- 731 Brainard, D. H. (1997). The Psychophysics Toolbox. *Spatial Vision*, 10(4), 433–436.
- 732 Breitmeyer, B. G. (2007). Visual masking: past accomplishments, present status, future
733 developments. *Advances in Cognitive Psychology*, 3(1-2), 9–20.
- 734 Celebrini, S., Thorpe, S., Trotter, Y., & Imbert, M. (1993). Dynamics of orientation coding in
735 area V1 of the awake primate. *Visual Neuroscience*, 10(5), 811–825.
- 736 Dobson, A. J., & Barnett, A. G. (2008). An introduction to generalized linear models (Third
737 Edition). Chapman & Hall/CRC.
- 738 Fabre-Thorpe, M., Richard, G., & Thorpe, S. (1998). Rapid categorization of natural images by
739 rhesus monkeys. *NeuroReport*, 9(2), 303.
- 740 Fee, M. S., Mitra, P. P., & Kleinfeld, D. (1996). Automatic sorting of multiple unit neuronal
741 signals in the presence of anisotropic and non-Gaussian variability. *Journal of Neuroscience*
742 *Methods*, 69(2), 175–188.
- 743 Glickfeld, L. L., Histed, M. H., & Maunsell, J. H. R. (2013). Mouse primary visual cortex is used
744 to detect both orientation and contrast changes. *Journal of Neuroscience*, 33(50), 19416–19422.
- 745 Hill, D. N., Mehta, S. B., & Kleinfeld, D. (2011). Quality metrics to accompany spike sorting of
746 extracellular signals. *Journal of Neuroscience*, 31(24), 8699–8705.
- 747 Histed, M. H., & Maunsell, J. H. R. (2013). Cortical neural populations can guide behavior by
748 integrating inputs linearly, independent of synchrony. *Proceedings of the National Academy of*
749 *Sciences*, 111(1), E178–87.
- 750 Häusser, M., & Smith, S. L. (2007). Neuroscience: controlling neural circuits with light. *Nature*,
751 446(7136), 617–619.
- 752 Jurjut, O., Georgieva, P., Busse, L., & Katzner, S. (2017). Learning Enhances Sensory
753 Processing in Mouse V1 before Improving Behavior. *The Journal of Neuroscience*, 37(27),
754 6460–6474.

- 755 Kawai, R., Markman, T., Poddar, R., Ko, R., Fantana, A. L., Dhawale, A. K., et al. (2015).
756 Motor cortex is required for learning but not for executing a motor skill. *Neuron*, 86(3), 800–
757 812.
- 758 Kovács, G., Vogels, R., & Orban, G. A. (1995). Cortical correlate of pattern backward masking.
759 *Proceedings of the National Academy of Sciences*, 92(12), 5587–5591.
- 760 Lamme, V. A. F., Zipser, K., & Spekreijse, H. (2002). Masking interrupts figure-ground signals
761 in V1. *Journal of Cognitive Neuroscience*, 14(7), 1044–1053.
- 762 Liang, F., Xiong, X. R., Zingg, B., Ji, X.-Y., Zhang, L. I., & Tao, H. W. (2015). Sensory Cortical
763 Control of a Visually Induced Arrest Behavior via Corticotectal Projections. *Neuron*, 86(3), 755–
764 767.
- 765 Lien, A. D., & Scanziani, M. (2013). Tuned thalamic excitation is amplified by visual cortical
766 circuits. *Nature Neuroscience*, 16(9), 1315–1323.
- 767 Macknik, S. L., & Livingstone, M. S. (1998). Neuronal correlates of visibility and invisibility in
768 the primate visual system. *Nature Neuroscience*, 1(2), 144–149.
- 769 Mazurek, M. E., & Shadlen, M. N. (2002). Limits to the temporal fidelity of cortical spike rate
770 signals. *Nature Neuroscience*, 5(5), 463–471.
- 771 Niell, C. M., & Stryker, M. P. (2008). Highly selective receptive fields in mouse visual cortex.
772 *Journal of Neuroscience*, 28(30), 7520–7536.
- 773 O'Connor, D. H., Hires, S. A., Guo, Z. V., Li, N., Yu, J., Sun, Q.-Q., et al. (2013). Neural coding
774 during active somatosensation revealed using illusory touch. *Nature Neuroscience*, 16(7), 958–
775 965.
- 776 Olsen, S. R., Bortone, D. S., Adesnik, H., & Scanziani, M. (2012). Gain control by layer six in
777 cortical circuits of vision. *Nature*, 483(7387), 47.
- 778 Otchy, T. M., Wolff, S. B. E., Rhee, J. Y., Pehlevan, C., Kawai, R., Kempf, A., et al. (2015).
779 Acute off-target effects of neural circuit manipulations. *Nature*, 528(7582), 358–363.
- 780 Paxinos, G., & Franklin, K. B. J. (2007). The Mouse Brain in Stereotaxic Coordinates (3rd ed.).
781 Elsevier Academic.

- 782 Peng, Y., Gillis-Smith, S., Jin, H., Tränkner, D., Ryba, N. J. P., & Zuker, C. S. (2015). Sweet and
783 bitter taste in the brain of awake behaving animals. *Nature*, 527(7579), 512–515.
- 784 Petruno, S. K., Clark, R. E., & Reinagel, P. (2013). Evidence that primary visual cortex is
785 required for image, orientation, and motion discrimination by rats. *PLoS ONE*, 8(2), e56543.
- 786 Poort, J., Khan, A. G., Pachitariu, M., Nemri, A., Orsolic, I., Krupic, J., et al. (2015). Learning
787 Enhances Sensory and Multiple Non-sensory Representations in Primary Visual Cortex. *Neuron*,
788 86(6), 1478–1490.
- 789 Prusky, G. T., & Douglas, R. M. (2004). Characterization of mouse cortical spatial vision. *Vision*
790 *Research*, 44(28), 3411–3418.
- 791 Reinhold, K., Lien, A. D., & Scanziani, M. (2015). Distinct recurrent versus afferent dynamics in
792 cortical visual processing. *Nature Neuroscience*, 18(12), 1789–1797.
- 793 Rolls, E. T., Tovee, M. J., & Panzeri, S. (1999). The neurophysiology of backward visual
794 masking: information analysis. *Journal of Cognitive Neuroscience*, 11(3), 300–311.
- 795 Rolls, E. T., Tovee, M. J., Purcell, D. G., Stewart, A. L., & Azzopardi, P. (1994). The responses
796 of neurons in the temporal cortex of primates, and face identification and detection.
797 *Experimental Brain Research*, 101, 473–484.
- 798 Romo, R., Hernández, A., Zainos, A., & Salinas, E. (1998). Somatosensory discrimination based
799 on cortical microstimulation. *Nature*, 392(6674), 387–390.
- 800 Salzman, C. D., Britten, K. H., & Newsome, W. T. (1990). Cortical microstimulation influences
801 perceptual judgements of motion direction. *Nature*, 346(6280), 174–177.
- 802 Shadlen, M. N., & Newsome, W. T. (1998). The variable discharge of cortical neurons:
803 implications for connectivity, computation, and information coding. *Information and*
804 *Computation*, 18(10), 3870–3896.
- 805 Tolhurst, D. J., Movshon, J. A., & Dean, A. F. (1983). The statistical reliability of signals in
806 single neurons in cat and monkey visual cortex. *Vision Research*, 23(8), 775–785.
- 807 Zhao, S., Ting, J. T., Atallah, H. E., Qiu, L., Tan, J., Gloss, B., et al. (2011). Cell type-specific
808 channelrhodopsin-2 transgenic mice for optogenetic dissection of neural circuitry function.
809 *Nature Methods*, 8(9), 745–752.

810 Zohary, E., Shadlen, M. N., & Newsome, W. T. (1994). Correlated neuronal discharge rate and
811 its implications for psychophysical performance. *Nature*, 370(6485), 140–143.

812

813

814

815

816

817

818

819

820

821

822

823

824

825

826

827

828

829

830

831

832

833

834 **Figure Legends**

835 **Figure 1. A virtual foraging behavior that depends on visual cortex.**

836 (A) Behavioral setup. The mouse is rewarded for stabilizing the target at the center of the
837 monitor for about a second. (B) Example session for a trained mouse. *Top*. Grey lines are
838 individual stimulus trajectories. Orange shaded area is the reward zone. Note different
839 trajectories of target versus distractor stimuli. *Bottom left*. Distribution of the times spent in the
840 reward zone for target (filled bars) and distractor stimuli (empty bars). *Bottom right*. The
841 probability that mice place the object in the reward zone for at least the minimal time for reward
842 (stop probability) depends on the identity of the grating. Here and further, error bars are 95%
843 confidence intervals. (C) Behavioral setup as above but visual cortex (VC) is silenced before the
844 appearance of the stimulus and for the duration of the trial on a randomly interleaved fraction of
845 trials. (D) Behavioral performance depends on contralateral VC. Same conventions as in (B).
846 *Top*. Example mouse. Stimulus trajectories during cortical silencing are in blue. This particular
847 mouse systematically overshot the reward zone when centering the target and subsequently
848 moved backwards to bring the target back in the reward zone. *Bottom left*. Distribution of times
849 spent in reward zone. Black: control; Blue: VC silencing. *Bottom right*. Stop probability under
850 control conditions (black) and during VC silencing (blue). Individual lines are individual mice
851 ($n=3$). (E) Behavioral performance is not affected by silencing ipsilateral VC. Same conventions
852 as in (D). (F) Visual cortex is not required to express the decision in a detection task. Mice
853 trained with one stimulus only (the target) are rewarded for stabilizing it at the center of the
854 monitor. *Top, Bottom left*. Example mouse. Stimulus trajectories during cortical silencing are in
855 blue. Same conventions as (B). A blank is defined as the absence of a target at regularly spaced
856 distances. *Bottom right*. Stop probability for 2 mice (individual lines).

857

858 **Figure 2. Lesion of visual cortex disrupts behavior.**

859 (A) Coronal brain sections showing the extent of lesion for an example mouse (black in (B) and
860 (C), 100 μ m sections, images of background fluorescence, see Methods for summary of all
861 mice). Outline of the different brain areas is from the Paxinos and Franklin brain atlas (Paxinos
862 & Franklin, 2007). Distances are relative to bregma. The retinotopic location in V1
863 corresponding to the stimulus in the initial 350 ms is ~ 3 mm from bregma and 2.3 mm from
864 midline. Note the absence of V1 (black). (B) Stop probability for the target and distractor
865 stimulus when mice performed the task (*left*) just before the lesion of visual cortex (day 0) or the
866 previous day (day -1) and (*right*) when mice performed the task 10 days after the lesion of visual
867 cortex. Individual lines are individual mice. Each color represents the same mouse in all panels.
868 All mice except the one displayed in grey had lesions in the left visual cortex (contralateral to the
869 stimulus); the one in grey had a lesion in the right visual cortex. Error bars are 95% confidence
870 intervals. (C) Stop probability for 3 of the mice in (B), (*left*) just before the gap in training (day
871 0), and (*right*) after the gap in training (day 17 or day 19 without training).

872

873

874

875

876

877

878

879

880 **Figure 3. Individual neurons can discriminate within 80 ms from onset of cortical response.**

881 (A) Experimental setup as in Figure 1A but with recording from primary visual cortex. (B)
882 Responses of two example units recorded simultaneously. *Top*. Raster plot. Black dots are action
883 potentials. *Bottom*. Peristimulus time histogram (PSTH). The number of action potentials per
884 trial is calculated in 25 ms bins. (C) Estimation of the onset of cortical response. The onset of
885 cortical response is defined for each mouse as the earliest deflection in the local field potential
886 following stimulus onset. Dashed lines indicate 3 standard deviations from baseline. Black
887 circles indicate onset of cortical response in 9 mice. Red circle and line are the mean and
888 standard deviation across mice. (D) Receiver operating characteristic (ROC) analysis for the 2
889 example units in (B). *Top*. Distribution of action potentials across trials for target (black bars)
890 and distractor stimuli (white bars) at 3 different intervals after the onset of cortical response.
891 *Bottom*. ROC curve for each graph on top. (E) Summary of areas under ROC for 72 units. Area
892 under ROC for individual units (individual lines) depends on the interval from cortical onset.
893 Black: example units in (C) and (D). For each unit at each interval starting at cortical response
894 onset, statistical significance for the separation of the distributions of the number of action
895 potentials for the target versus distractor was assessed using Wilcoxon ranksum test and the
896 Benjamini-Hochberg correction for multiple comparisons ($p<0.012$). (F) The fraction of
897 discriminating units discriminating at a particular interval increases with increasing time from
898 cortical response onset. A unit is defined as discriminating if by 300 ms $p<0.012$.
899 (G) Experimental set up as in (A) but stimulus position is always fixed, mouse is not rewarded,
900 and the grating is drifting. Grey lines are orientation tuning curves for individual discriminating
901 units preferring the target (top) or the distractor (bottom) during the task. Colored line is the
902 mean across units. (H) The area under ROC over the initial 80 ms after cortical onset during the
903 task is plotted against the difference in the number of action potentials in response to passively
904 viewed stimuli of 45° and 90°. Circles are individual discriminating units ($p>0.012$, Wilcoxon
905 ranksum test) that prefer target (red) or distractor (black). R^2 is the fraction of the variance
906 explained by the linear fit to the data.

907

908

909 **Figure 4. It takes visual cortex 80 ms to enable perceptual discriminations.**

910 **(A)** *Left:* Experimental setup. *Right:* Arrows indicate the onset of LED illumination. Each
911 interval was tested in separate behavioral sessions. **(B)** Example mouse. Stimulus trajectories
912 during cortical silencing (blue) and under control conditions (gray) for three different LED
913 illumination onset latencies (40 ms; 80 ms; 300 ms) relative to the onset of the cortical response.
914 Individual lines are individual trials. **(C)** Summary of stopping probability for 8 mice. Black:
915 control; Blue: cortical silencing. Times indicate the LED illumination onset after onset of the
916 cortical response. Individual lines are individual mice. Error bars are 95% confidence intervals.
917 Note that behavioral performance during cortical silencing increases with increasing LED onset.
918 **(D)** Probability of a correct choice during cortical silencing (blue) depends on the onset of LED
919 illumination relative to the onset of the cortical response. Individual lines are individual mice.
920 Black circles indicate probability correct for individual mice for trials with no cortical silencing.

921

922 **Figure 5. Discrimination accuracy when V1 is active for only 80 ms is sensitive to the**
923 **difficulty of the task.**

924 (A) Experimental setup as in Figure 4A. (B) Probability of a correct choice for (*top*) control trials
925 and for (*bottom*) trials with cortical silencing for 3 mice first trained in the main task (blue,
926 target: 90°, distractor: 45°) and then in the harder discrimination task (red, target: 60°, distractor:
927 45°). Error bars are 95% confidence intervals. Asterisks indicate significant difference in the
928 choice accuracies in the two tasks ($p=0.001-0.018$, Wilcoxon ranksum test on choice data). (C)
929 Stop probability for the target stimulus (T) and the distractor stimulus (D) for 2 intervals from
930 (B), *left*, when cortex is silenced at 80 ms or, *right*, 140 ms following onset of cortical response.

931

932

933

934

935

936

937

938

939

940

941

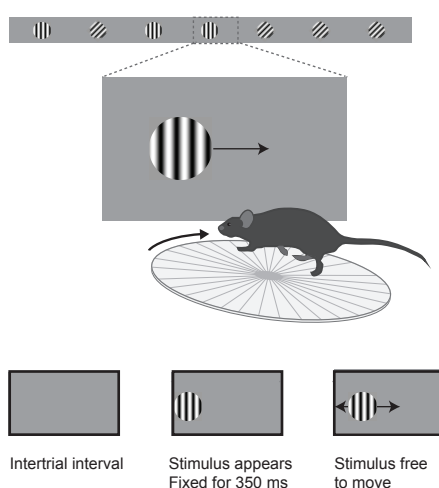
942

943 **Figure 6. Neurons usually fire only their first action potential in the initial 80 ms.**

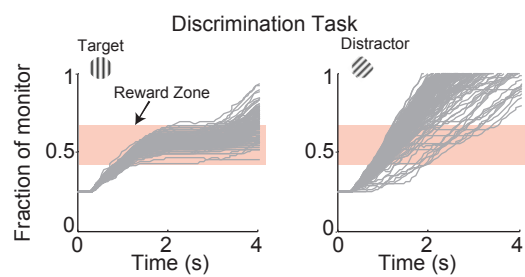
944 (A) Experimental setup as in Figure 3A. (B) Raster plot (APs, black dots) for an example unit for
945 preferred (*left*) versus the non-preferred stimulus (*right*). Red circles indicate the first AP in each
946 trial after the onset of the cortical response. (C) The distribution of times of the first AP for
947 individual discriminating units (grey circles, time bins of 20 ms) for those trials in which the first
948 AP occurred within the initial 300 ms following the onset of the cortical response, for (*left*) the
949 preferred and (*right*) the non-preferred stimulus. Black line is the mean across units. Red circle
950 and line through are the median and SEM, respectively. (D) Mean of times of the first AP across
951 trials for individual discriminating units (circles; same trials and window as in C) plotted for the
952 preferred stimulus versus the non-preferred stimulus. *Top*. Distribution of the mean times for the
953 preferred stimulus. *Left*. Distribution of the mean times for the non-preferred stimulus. Red circle
954 and line through are the median and SEM, respectively. *Left panel*. Distribution of the difference
955 in the mean time of the first AP for the preferred and the non-preferred stimulus for all
956 discriminating units. Red circle and line through are the median and SEM, respectively. (E) The
957 distribution of the number of APs across trials for the preferred stimulus for the initial 80 ms
958 after cortical onset for (*left*) the example unit in (B) and for (*right*) all discriminating units
959 approximates a Poisson distribution predicted from the mean number of APs (red line). (F) *Left*
960 *panel*. The distribution of the number of action potentials (mean across trials) across
961 discriminating units is shown for the preferred stimulus over the initial 80 ms (black) and 300 ms
962 (grey). Last bin also includes units that fired more than 5 APs. Circle and line through are the
963 median and SEM, respectively. *Right panel*. The number of APs (mean across trials) for
964 individual discriminating units (circles) for the preferred versus the non-preferred stimulus over
965 the initial 80 ms (black) and the initial 300 ms (grey). (G) Area under ROC for individual units
966 (individual lines), based only on the first AP after cortical onset on each trial plotted against the
967 interval from the onset of the cortical response. Statistical significance was assessed same as in
968 Figure 3E. (H) Fraction of discriminating units discriminating depends on the interval from
969 cortical onset. A unit is defined as discriminating if by 300 ms p<0.013.
970

Figure 1

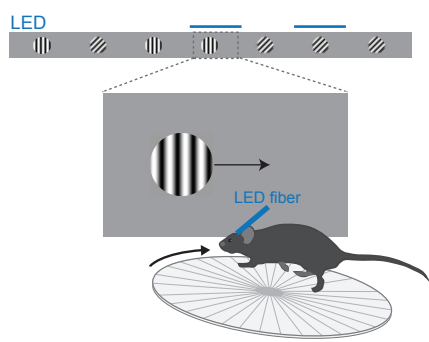
A



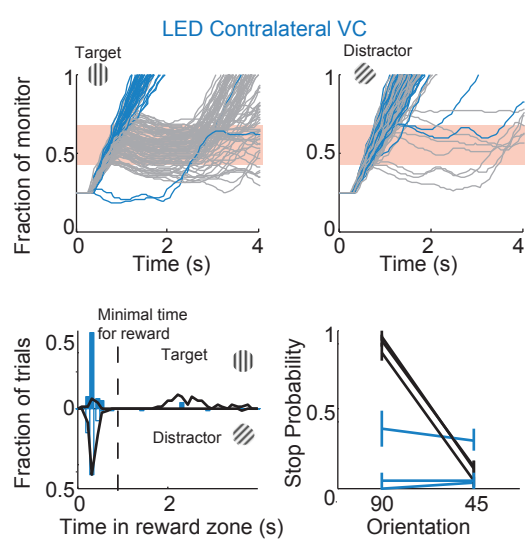
B



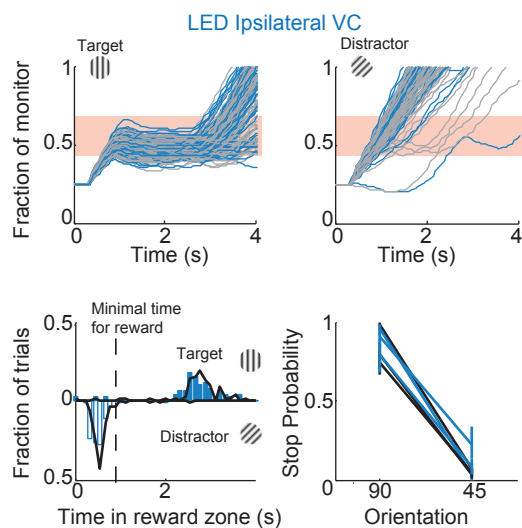
C



D



E



F

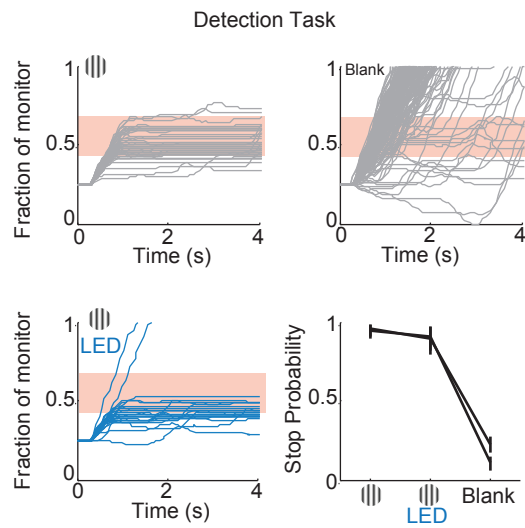


Figure 2

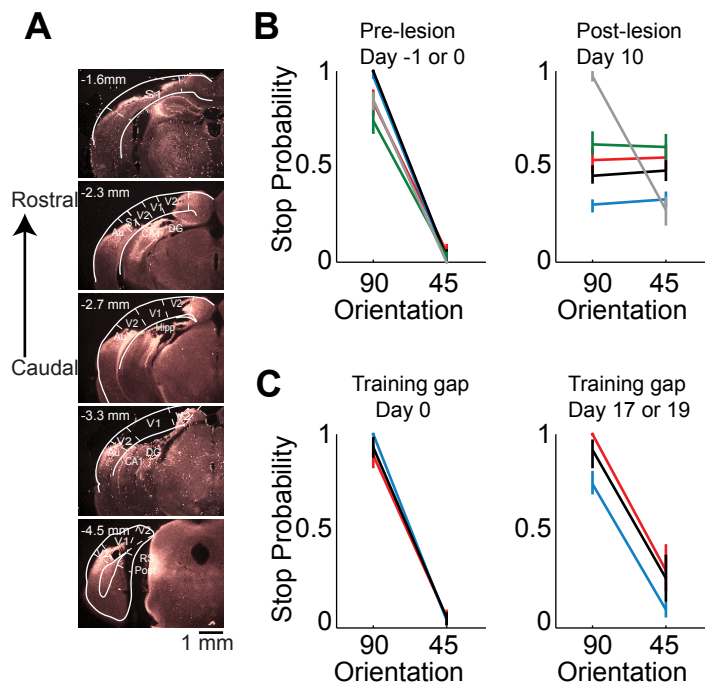
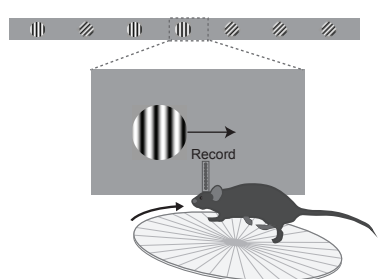
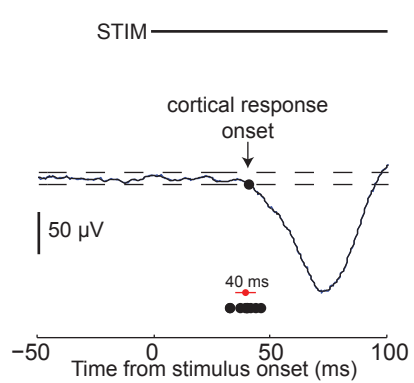


Figure 3

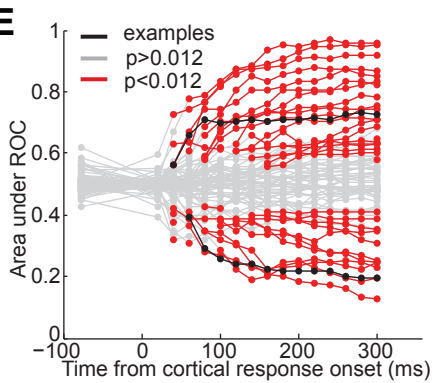
A



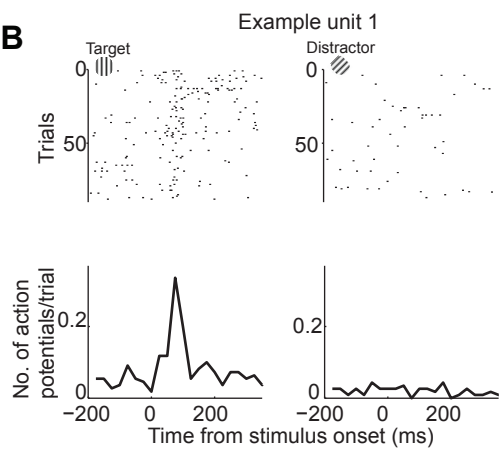
C



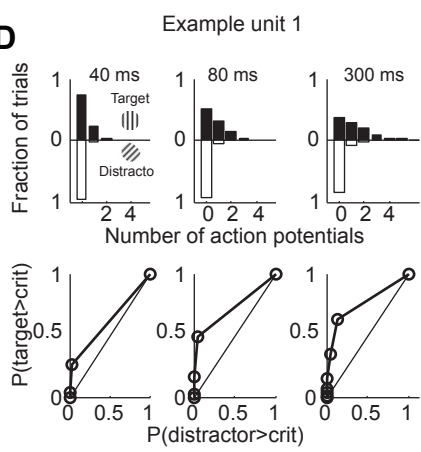
E



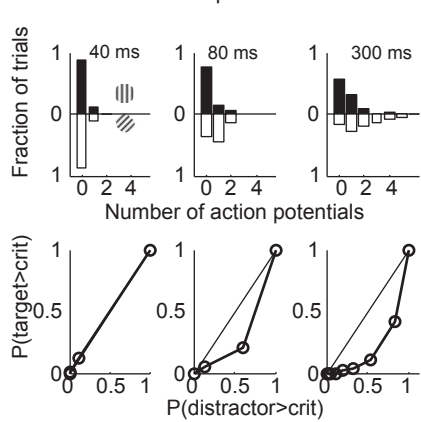
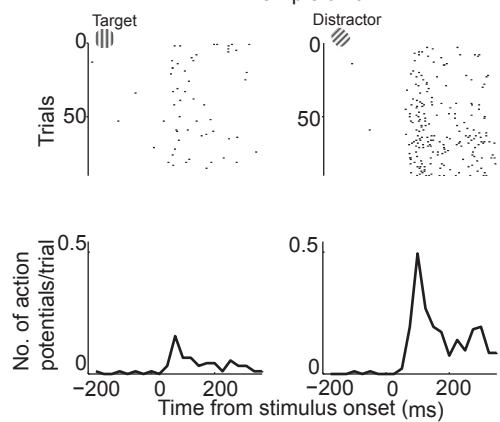
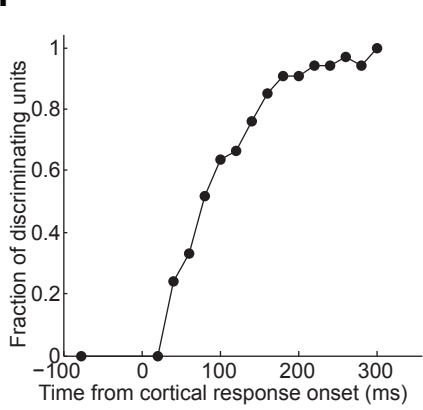
B



D



F



G

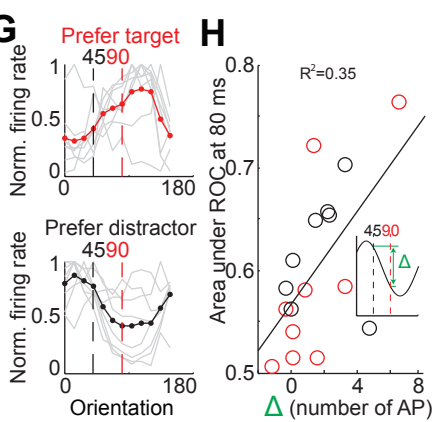


Figure 4

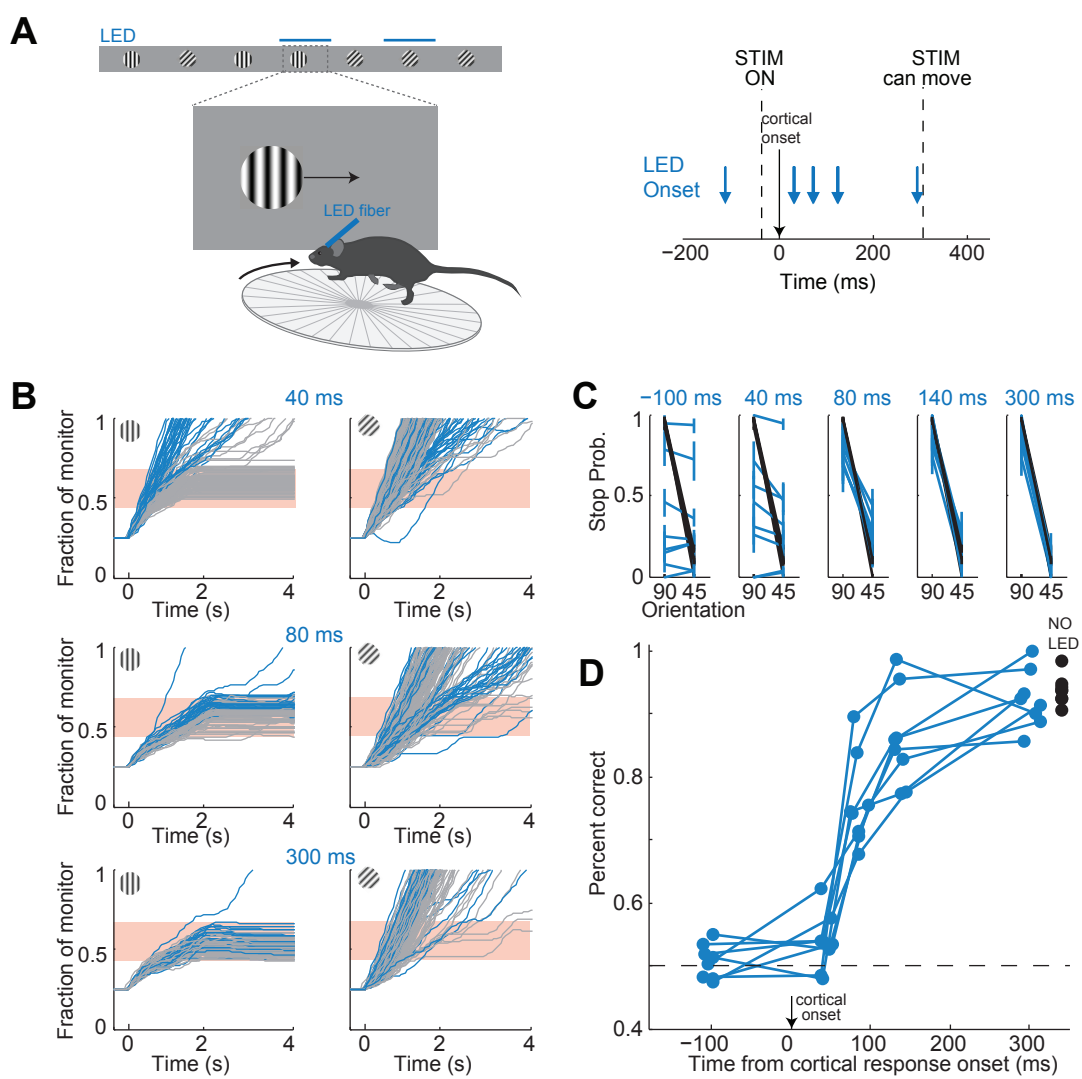


Figure 5

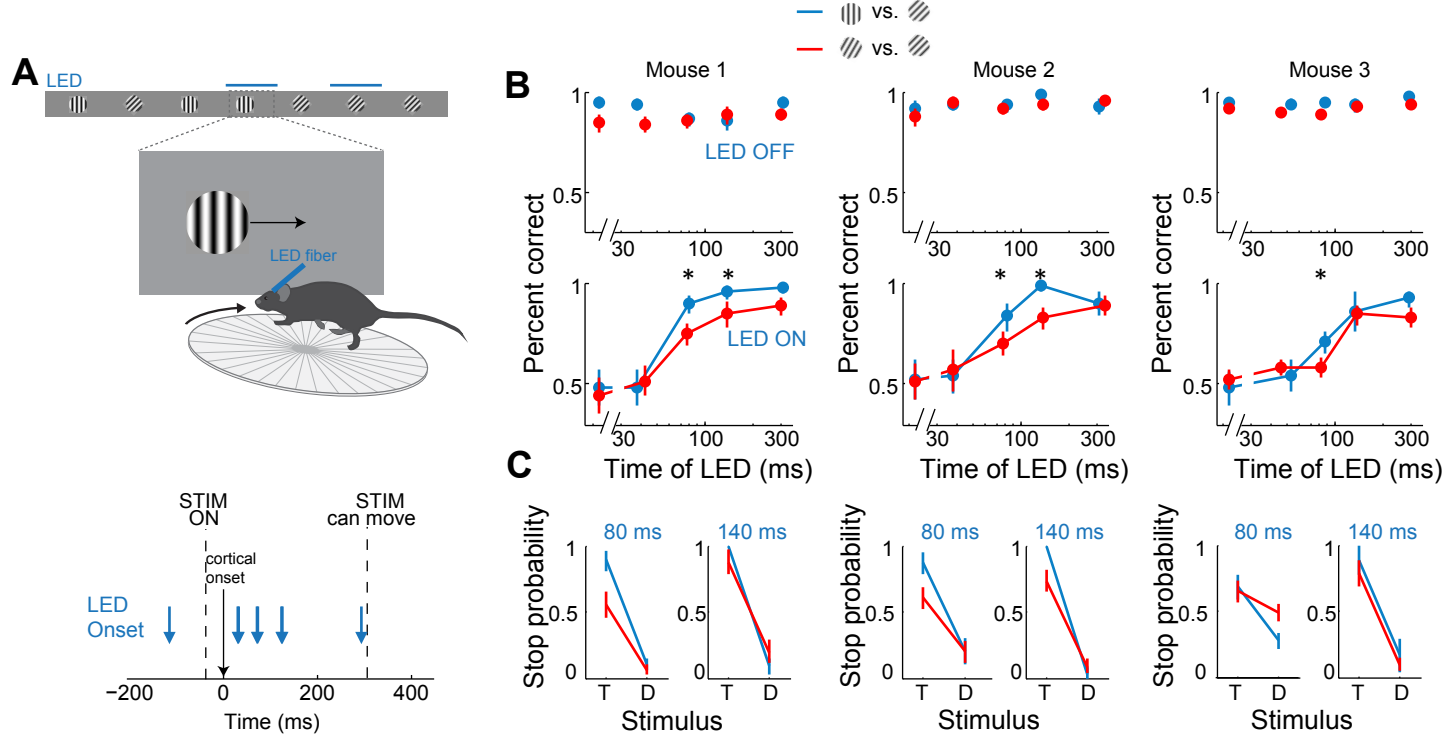
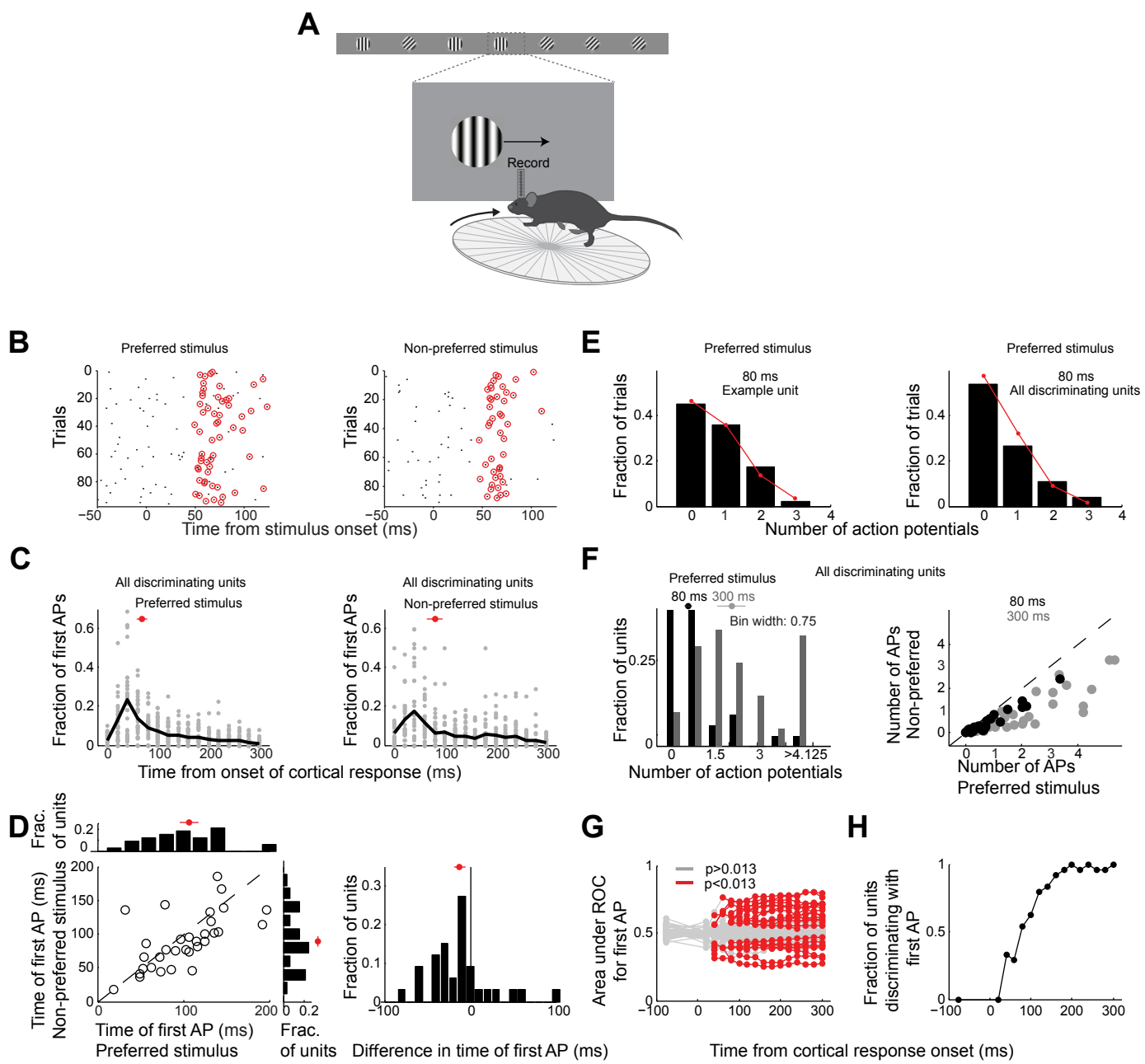
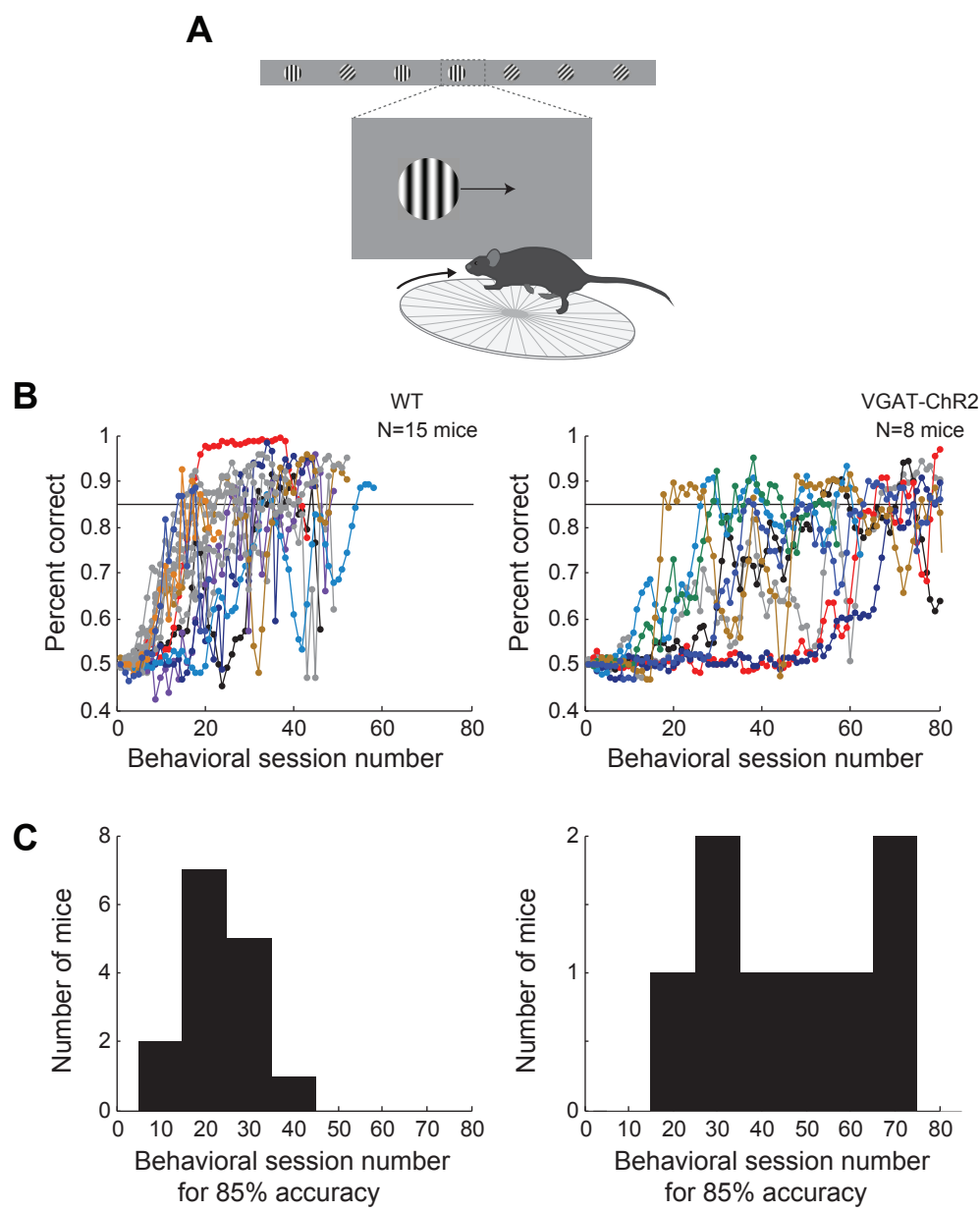


Figure 6

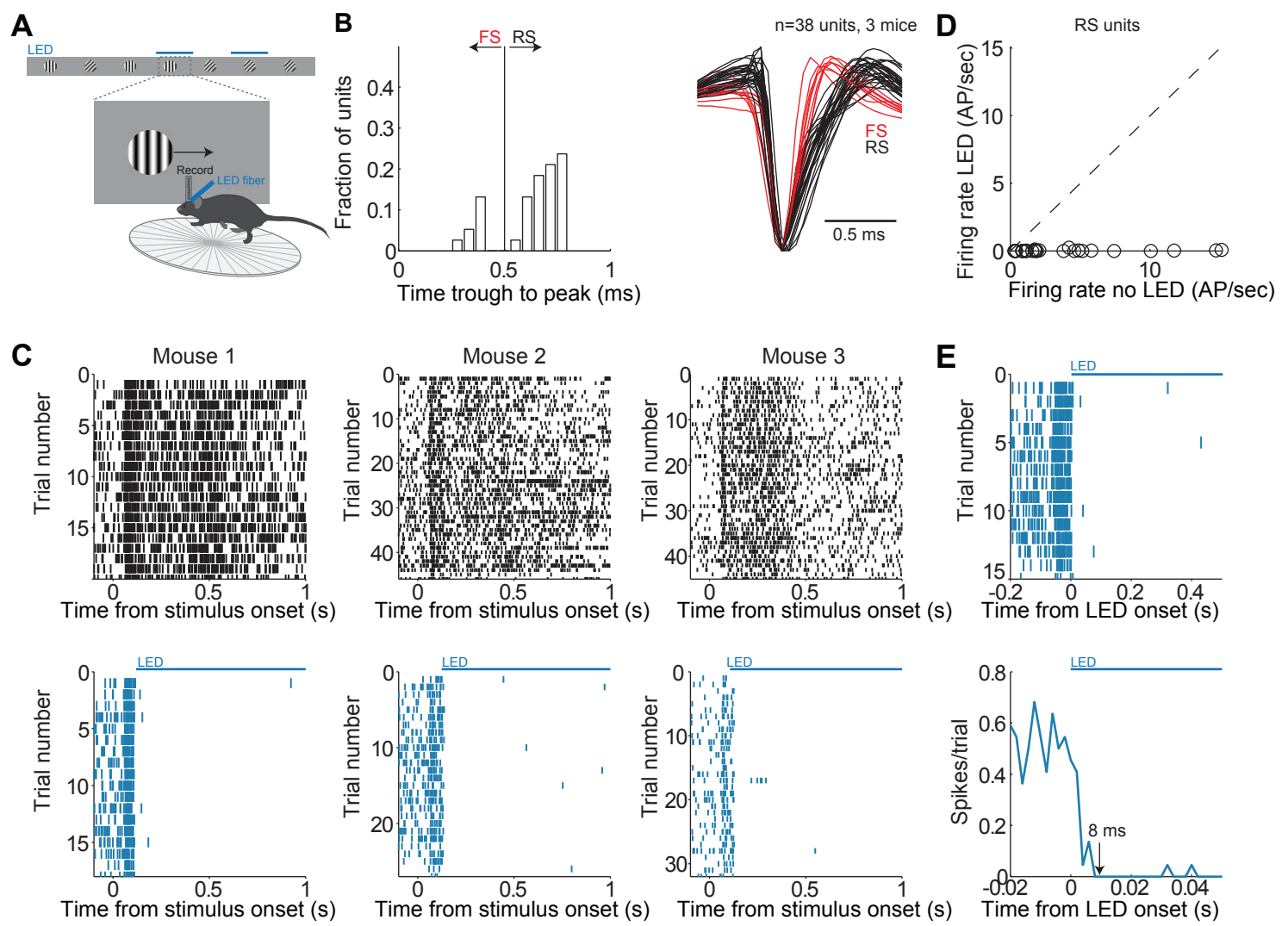


Supplementary Figure 1



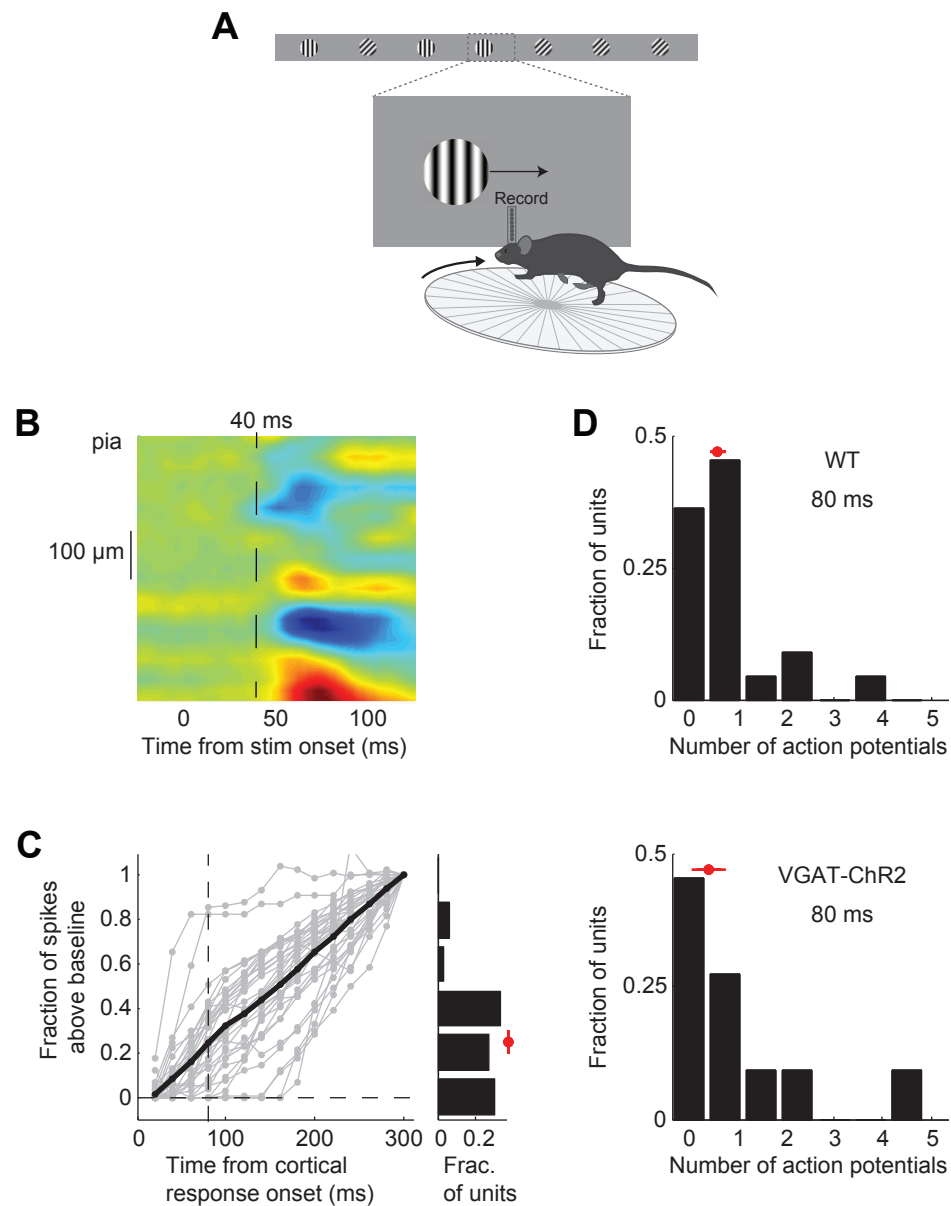
Supplementary Figure 1. Learning curves for wild type and transgenic mice. (A) Behavioral setup. (B) Probability of a correct choice for the different behavior sessions over the course of training for wild type mice (left, subset of mice trained for subsequent electrophysiology recordings, all mice shown in the main figures are included) and transgenic mice (right, subset of mice trained for subsequent optogenetic silencing or electrophysiology recordings, 8/9 mice shown in the main figures are included; for 1/9 mice the initial training data was corrupted). Sessions lasting <10 min were excluded. Probability of a correct choice for a given session is the average of the probability of a correct choice in a 3-session sliding window centered on the shown trial. Individual lines are individual mice. (C) Distribution of the number of training sessions that it takes mice to reach an overall accuracy of 85% correct.

Supplementary Figure 2



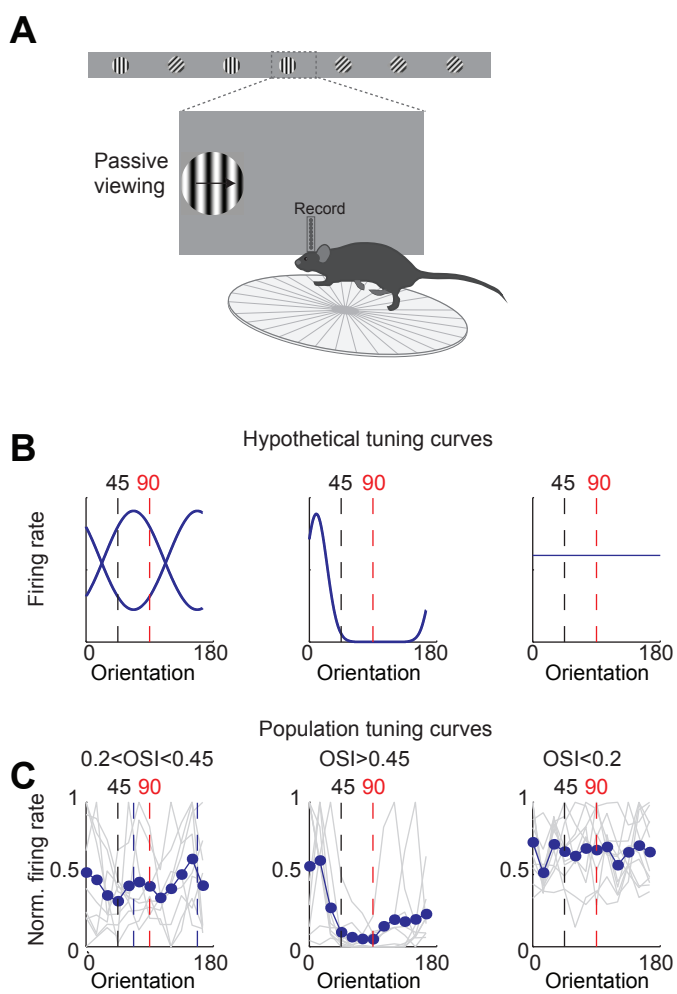
Supplementary Figure 2. Reversible, rapid and complete silencing of V1. (A) Experimental set up as in Figure 1C. (B) Distribution of the time from trough to peak in the average waveform of the action potential across single units ($n=3$ mice). Single units are labelled as regular spiking (RS, black lines) or fast spiking (FS, red lines) depending on their time of trough to peak. (C) Reversible and complete silencing of V1. *Top*. Raster plots (each dot is an action potential) for 3 mice including all isolated single units (all layers) for trials under control conditions (no LED) aligned at stimulus onset. *Bottom*. Same as above but for trials with LED illumination. LED and control trials were randomly interleaved. LED onset was approximately at 120 ms after stimulus onset. (D) Firing rate of individual RS units computed from 130 ms to 1 sec following stimulus onset under control conditions plotted against firing rate during LED illumination. (E) Rapid silencing of V1. *Top*. Raster plot (each dot is an action potential) for all RS units from all 3 mice for trials with LED illumination aligned at the time of LED onset. *Bottom*. Peri-event time histogram from all isolated single units (2 ms bins) for trials with LED illumination. Arrow indicates time when the firing rate drops to zero.

Supplementary Figure 3



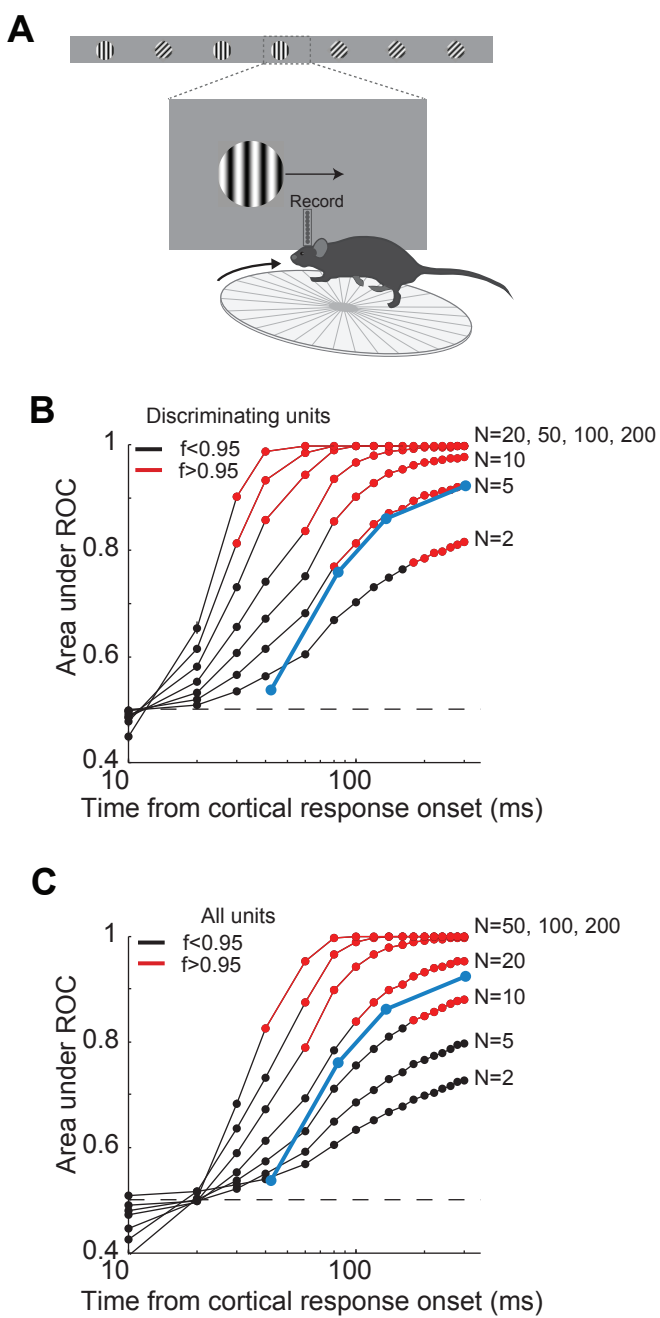
Supplementary Figure 3. Characterization of V1 recordings during behavior. (A) Experimental setup as in Figure 3A (B) Average current source density for 5 mice (see Methods). Blue indicates current sinks; red indicates current sources. The top sink is layer 4. 40 ms indicates the average onset of the cortical response across mice (see Figure 3C). (C) Fraction of stimulus elicited spikes at different time intervals relative to 300 ms following onset of cortical response. Grey lines are individual discriminating units; black line is the mean. If a unit was suppressed below baseline, the value for spikes above baseline was set to zero. Vertical dotted line marks 80 ms. *Right*. Distribution of the fraction of stimulus elicited spikes at 80 ms following onset of cortical response for all discriminating units. By 80 ms discriminating units fire $25 \pm 4\%$ of the total spikes. (D) Distribution of the number of action potentials fired over the initial 80 ms following onset of the cortical response for discriminating units recorded from wild type mice (*top*, n=5 mice) or VGAT-ChR2 mice (*bottom*, n= 4 mice). The two distributions are not significantly different ($p=0.95$, Wilcoxon rank sum test). Red circle and line through it indicate median and sem, respectively.

Supplementary Figure 4



Supplementary Figure 4. Tuning curves for units that do not discriminate. (A) Experimental set up as in Figure 3A but the stimulus position is always fixed, mouse is not rewarded, and the grating is drifting. (B) Example hypothetical tuning curves for units that do not discriminate. *Left*. Peak of tuning curve is in the middle of distractor (45°) and target (90° ; i.e. 67.5° and 157.5°). *Middle*. Narrow tuning curve with peak away from 45° and 90° . *Right*. Flat tuning curve. (C) Population tuning curves. Individual units (grey lines) were grouped according to their orientation selectivity index (OSI). Blue lines are the population mean.

Supplementary Figure 5



Supplementary Figure 5. Comparison of neural and behavior discrimination. (A) Experimental setup as in Figure 3A. (B) Area under ROC curve as a function of time from cortical onset for a 'pooling neuron', which for each trial has all the spikes of N units that are randomly drawn from a pool of all discriminating units (see Methods). Each line is the average of the areas under ROC for 10 different pools of discriminating units. Errorbars are sem. For each area under ROC curve, at each interval, statistical significance for the separation in the distribution of number of action potentials for the target versus the distractor was assessed using Wilcoxon ranksum test ($p<0.05$). f is at each time interval the fraction of 'pooling neurons' with $p<0.05$. Blue line is the average probability of a correct choice for all the mice in Figure 4D. (C) Same as D but for all units.

Supplementary Table 1

| MOUSE | STRAIN | EXPERIMENT | HOLD TIME | TRACK GAIN | TARGET PROBABILITY |
|-------|-----------|-------------------------------------|----------------------|------------|--------------------|
| 1 | VGAT-ChR2 | Optogenetic silencing | 0.6 sec | 0.45 | 0.33 |
| 2 | VGAT-ChR2 | Optogenetic silencing | 0.9 sec | 0.6 | 0.5 |
| 3 | VGAT-ChR2 | Optogenetic silencing Physiology | 0.9 sec 0.6 sec | 0.6 0.6 | 0.33 0.50 |
| 4 | VGAT-ChR2 | Optogenetic silencing | 1.0 sec | 0.35 | 0.33 |
| 5 | VGAT-ChR2 | Optogenetic silencing | 1.0 sec | 0.3 | 0.25 |
| 6 | VGAT-ChR2 | Optogenetic silencing | 1.0 sec | 0.6 | 0.33 |
| 7 | VGAT-ChR2 | Optogenetic silencing Physiology | 0.75 sec 1.10 sec | 0.3 0.3 | 0.33 0.50 |
| 8 | VGAT-ChR2 | Optogenetic silencing Physiology | 0.9 sec 0.7 sec | 0.3 0.3 | 0.5 0.5 |
| 9 | VGAT-ChR2 | Physiology | 1.0 sec | 0.2 | 0.5 |
| 10 | WT | Physiology | 0.9 sec | 0.35 | 0.5 |
| 11 | WT | Physiology | 1.1 sec | 0.35 | 0.5 |
| 12 | WT | Physiology | 0.6 sec | 0.35 | 0.5 |
| 13 | WT | Physiology | 0.6 sec | 0.5 | 0.5 |
| 14 | WT | Physiology | 1.1 sec | 0.3 | 0.5 |
| 15 | WT | Cortical ablation | 1.3 sec | 0.35 | 0.5 |
| 16 | WT | Cortical ablation | 0.9 sec | 0.3 | 0.5 |
| 17 | WT | Cortical ablation | 1.3 sec | 0.3 | 0.5 |
| 18 | WT | Cortical ablation | 0.9 sec | 0.3 | 0.5 |
| 19 | WT | Cortical ablation | 0.9 sec | 0.3 | 0.5 |

Supplementary Table 1. Parameters for the behavioral task for each of the mice included in the main experiments. Hold time is the minimal time that the target stimulus has to spend in the reward zone for a reward to be available. Track gain is the stimulus displacement on the monitor (cm) / running distance (cm). Target probability is the fraction of stimuli that are the target stimulus (stimuli are randomly interleaved).